



# Watershed prioritization using morphometric analysis and vegetation index: a case study of Huehuetan river sub-basin, Mexico

Adolfo López-Pérez<sup>1</sup> · Demetrio S. Fernández-Reynoso<sup>1</sup>

Received: 3 March 2020 / Accepted: 3 August 2021 / Published online: 21 August 2021  
© Saudi Society for Geosciences 2021

## Abstract

Soil degradation is one of the most important issues all over the world. Characterizing and describing a watershed is key to develop action plans that prevent soil degradation. Morphometric analysis and its quantitative description are commonly used to describe a watershed and its drainage system; however, these methodologies are long, and their accuracy can be contested. In this paper, we present an alternative for watershed prioritization by coupling principal component analysis (PCA) with geographic information systems (GIS) for watershed prioritization using morphometric parameters and land cover with Normalized Difference Vegetation Index (NDVI). We use data of the Huehuetan river sub-basin, in Chiapas, Mexico, to operationalize our methodology. We found that the principal components (PC01, PC02, and PC03) had a variance more than the 92% in relation to morphometric parameters such as stream frequency ( $F_s$ ), drainage density ( $D$ ), elongation ratio ( $R_e$ ), and drainage texture ( $D_t$ ). The highest priority was found in the upper part of the sub-basin; watersheds 07, 08, and 06 had the 1<sup>st</sup>, 2<sup>nd</sup>, and 3<sup>rd</sup> priority ranks, respectively, reflecting the importance to establish preventive and corrective measurements to reduce soil degradation and mitigate the effects in lower parts of the sub-basin. From our research, we concluded that the use of PCA is a good tool to discriminate the insignificant parameters from the analysis and improve quality of results. In addition, our methodological proposal saves time on the analysis of morphometric parameters and together with NDVI could be a good methodology for watershed prioritization in tropical and sub-tropical areas like basins located in the southeast part of Mexico.

**Keywords** Morphometric analysis · Soil degradation · Sub-basin · PCA · Watershed prioritization · NDVI

## Introduction

Soil degradation is one of the most important degradation processes all over the world; annually tons of soils are lost by water erosion, land use change, and inadequate management practices, causing an irreversible damage in agricultural and mountain areas (Prieto-Amparán et al. 2019). A good soil and water management is essential to prevent soil degradation, and several countries are developing river basin management plans to help solve the problem by using watershed

prioritization's methodologies (Javed et al. 2009). For a good soil and water management in a given area, it is crucial to characterize a watershed or basin and its drainage system because it helps to estimate how much water runs downstream, how much soil gets lost, and what measures can be applied (Eze and Efiog 2010), information useful for sustained soil and water development, conservation, and restoration.

In this paper, we define a watershed as an area that drains the entire rainfall into a particular stream outlet (Chopra et al. 2005; Pal et al. 2012). In this area, different hydrological, geological, and structural processes interact with each other, and those processes are relevant for water erosion, soil evolution and properties, and biodiversity management. Those processes have a close relationship with the morphometry of the watershed (Hajam et al. 2013) and are directly associated with surface runoff and its hydrological response (Price 2011; Méndez 2016).

Characterizing and describing a watershed and its drainage system through a morphometric analysis and quantitative

---

Responsible Editor: Amjad Kallel

✉ Demetrio S. Fernández-Reynoso  
demetrio@colpos.mx

<sup>1</sup> Graduate Studies in Water Sciences, Colegio de Postgraduados, Campus Montecillo, Texcoco, State of Mexico 56230, Mexico

description is relevant because these parameters show the evolution of the drainage system and the relationship between processes associated with soil degradation (Strahler 1964). The morphometric parameters and land cover are a prerequisite for watershed prioritization when trying to implement soil and water conservation measurements or for developing watershed management plans.

The morphometric parameters are the most important characteristics used to analyze a watershed because they can provide quantitative information (Ramu and Mahalingam 2012). Several studies (Horton 1945; Miller 1953; Nag 1998; Migiros et al. 2011) have shown that the morphometry of a watershed is affected by the interrelation of the architecture of the drainage network and factors such as climate, geology, relief, and structural forms of a basin. The use of basin's morphometry as a methodology is not new, several authors (Horton 1932, 1945; Smith 1950; Miller 1953; Strahler 1964) have pioneered research on basin's morphometry, but other methods that are more precise continue to be explored. Most recently, similar works to morphometric analysis have been carried out using geographic information systems (GIS) and remote sensing (RS) to assess morphological features and analyze basins' properties in a more reliable and precise way (Nag and Chakraborty 2003; Rudraiah et al. 2008; Magesh and Chandrasekar 2012; Sharma et al. 2015; Resmi et al. 2019). In addition, statistical analysis and multicriteria analysis have been included to analyze some of the morphometric parameters by using different methodologies like principal component analysis (PCA) (Khanchoul and Saaidia, 2017; Meshram and Sharma, 2018), fuzzy analytical hierarchy process (Ahmed et al. 2018), and analytic network process (Chowdary et al. 2013; Gopinath et al. 2016), offering useful results for decision-makers. Another important factor to characterize a basin is its land use degradation because of the crucial role of vegetation cover on the response of a watershed to different rainfall events. The spatial distribution of vegetation cover—based on NDVI variation—can be used as indicator for basin degradation degree, and it helps to determine critical areas for soil conservation and vegetation cover restoration.

In understanding the performance of a watershed and the prioritization of the morphometric parameters and the NDVI, the analysis and process can be improved by using other techniques like principal component analysis (PCA) (Ahmed et al. 2018), because they reduce the number of variables to be used, i.e., from using all the variables to only use the most significant ones to the degradation processes. The easy access to data sources to get morphometric parameters and Normalized Difference Vegetation Index (NDVI) makes them good methods for watershed prioritization coupled with PCA reducing time while also increasing quality in the results.

Particularly in Mexico, researchers have come up with alternative methodologies for watershed prioritization.

However, most of these methodologies have been developed for arid and semi-arid conditions. For example, in the northern part of Mexico, some researches have been using methodologies like overlay maps (Martínez-Ramírez et al. 2017), weighted sum (Olguín-López and Pineda-López 2010), and multicriteria analysis (Zarco-Arista et al. 2010), but conditions in those areas are mostly arid (the rainiest month could be 60 mm), and therefore, variables are different and do not apply to cases with high precipitations and extreme events.

In this paper, specifically, we present an alternative methodology for watershed prioritization using morphometric analysis and NDVI coupled with PCA and GIS in Mexico mainly in tropical and sub-tropical lands by using variables with high impact (selected by PCA) on soil degradation. With our work, we present an alternative methodology for watershed prioritization for areas with high precipitation and extreme rainy events aiming to fill this methodological gap.

We use the case of the Huehuetan river sub-basin to develop our methodological proposal and test it. The Huehuetan river sub-basin is located in the southeast part of Mexico, in the state of Chiapas, where high precipitation occurs even extreme events like hurricanes (the rainiest month could be 550 mm) (Baumann and Arellano 2003). These particular conditions of high precipitation and extreme events require specific methodologies to prioritize watersheds based on statistical methods like PCA where variables can be discretized and considering only those that have greater influence on degradation processes.

## Materials and methods

### Study area

The Huehuetan river basin is located at the southeast region of the Mexican state of Chiapas, near to the border with Guatemala (Fig 1), covering up to 752.42 km<sup>2</sup> and emptying into the Pacific Ocean. In this study, we analyzed the upper part of the basin where a rain gauge station called Huehuetan is located (−92° 24' 02.43" W, 15° 00' 05.38" N), covering an area of 319.27 km<sup>2</sup>. We divided the Huehuetan river sub-basin into eight watersheds assessed through the SWAT model (*Soil and Water Assessment Tool*) using a digital elevation model (DEM) with a resolution of 15 m per pixel. The watersheds were classified using the Pfafstetter methodology (Verdin and Verdin 1999), and the drainage network was categorized by Strahler's order methodology (Strahler 1957).

The Huehuetan river sub-basin is part of the Sierra Madre de Chiapas and has a steep relief in its upper part. The 83.15% of the basin had slopes greater than 10%, and elevations vary between 30 and 2690 m above mean sea level (Fig 2); this abrupt topography and intense rainfall episodes favor extreme hydro-meteorological events with large volumes of runoff,

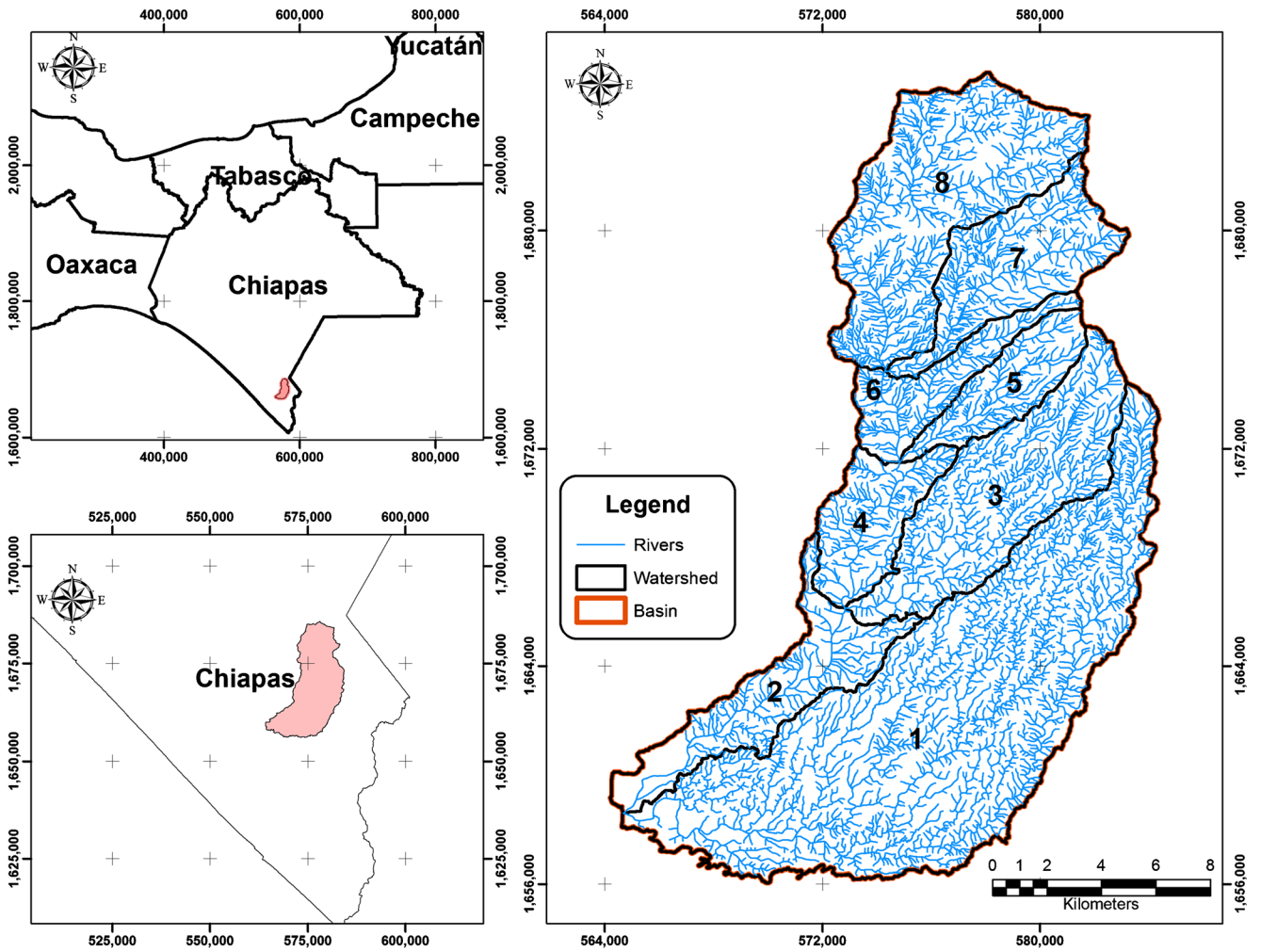


Fig. 1 Location of the Huehuetan river sub-basin and delineated watersheds

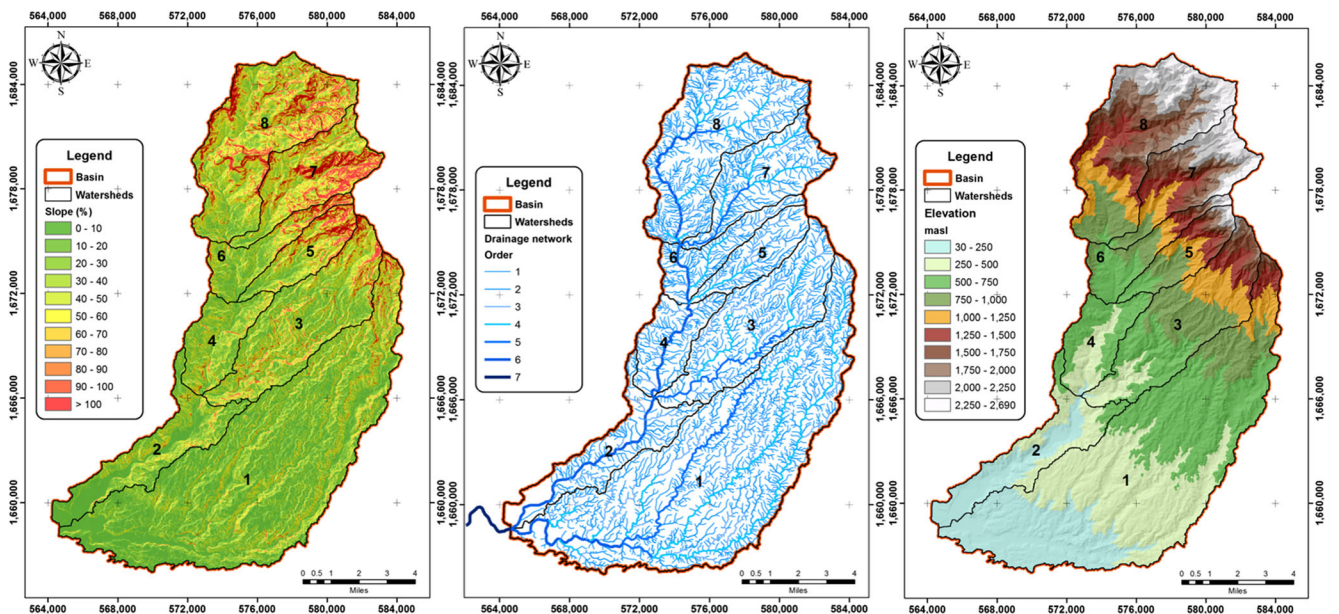


Fig. 2 Spatial distribution of the slope, drainage network, and elevations in the Huehuetan river sub-basin

soil erosion on hillslopes, sediment transport on channels, and mass movements due to soil saturation. The annual precipitation varies from 1200 mm in the lower part to more than 3500 mm in the middle and upper areas of the sub-basin from May to October mainly and being September the rainiest month with 550 mm on average. Lithosols soils are the largest soil unit in the area, followed by Andisols, Cambisols, and Luvisols. When frequent rainfall occurs, these soils generate large volumes of surface runoff, affect the water infiltration capacity, and cause soil pore saturation and landslides on steeper slopes.

### Data source

In this study, we used a digital elevation model with a resolution of 15 m per pixel provided by the continuous Map of Mexican Elevations (CEM 3.0), downloaded in the official website of the National Institute of Geography and Statistics (<https://www.inegi.org.mx/app/geo2/elevacionesmex/>). The NDVI was calculated by using a satellite image of the LANDSAT 8 Satellite, downloaded at the official website of the US Geological Survey (<https://earthexplorer.usgs.gov/>) and considering bands 4 (Red) and 5 (Infrared) in the following equation (1):

$$\text{NDVI} = \frac{B5 - B4}{B5 + B4} \quad (1)$$

### Determination of morphometric parameters using geographical information systems

We determined the morphometric parameters for each watershed using the formulas described in Table 1. Some parameters were generated with GIS tools. The hypsometric integral (HI) and the hypsometric curve (HC) were calculated with the CalHypso tool (Pérez-Peña et al. 2009) using equations adjustment (2 and 3) proposed by Strahler (1952) and Harlin (1978). The hypsometric curve was classified according to Strahler's methodology (Strahler 1952).

$$f(x) = a + bx + cx^2 + dx^3 \quad (2)$$

$$\left(\frac{h}{H}\right)_i = a_i + b_i\left(\frac{a}{A}\right) + c_i\left(\frac{a}{A}\right)^2 + d_i\left(\frac{a}{A}\right)^3 \quad (3)$$

### NDVI values for the Huehuetan watersheds

The NDVI values were calculated from the LANDSAT 8 OLI satellite image retrieved on December 25, 2018. The resulting values were grouped according to the classification shown in

Table 2 and which was done by Gómez-Almonte (2005) and Merg et al. (2011).

### Principal component analysis

Multivariate analysis is a technique that identifies common patterns in the distribution of data and reduces the size of the initial matrix to facilitate its interpretation. The PCA was used to know the contribution of morphometric parameters to the soil degradation process and which of those parameters have greatest influence in soil degradation. The correlations generated by PCA allow to look closely at the information contained in multiple variables, and they help to reduce variables redundancy (Sharma et al. 2015; Meshram and Sharma 2018). Since the PCA technique depends on the total variance from the original variables, it is most suitable when all variables are using the same measurement units. Hence, it is necessary to express the variables in standard form, i.e., selecting the unit of measurement for each variable so the sample variance is 100%. Singh et al. (2009) summarize the PCA analysis in three steps:

1. Calculate the correlation matrix,  $R$ .
2. Calculate the principal component loading matrix by PCA.
3. In the principal component (PC) loading matrix, Eigenvalues greater than one indicate significant PC loading.

While using a correlation matrix allows to numerically affirm the degree of association between pairs of variables, it does not allow to link these variables directly to a particular parameter. On the contrary, a PC loading matrix determines a matrix of loadings and how they associated with a particular parameter (Farhan et al. 2017). To obtain the statistical values, principal components, and Eigenvalues, the RStudio software and the FactoMineR package were used (Lê et al. 2008).

### Watershed prioritization

The values of the morphometric parameters for each watershed were determined and classified considering the following assertions (Javed et al. 2009; Londhe et al. 2010; Kanth and Hassan 2012; Tolessa and Rao 2013). The linear parameters that have direct relationship with watershed erodibility, drainage system amplitude, and dissection are watershed area ( $A$ ), drainage density ( $D$ ), stream frequency ( $F_s$ ), drainage texture ( $D_t$ ), form factor ( $F_f$ ), mean bifurcation ratio ( $R_{bm}$ ), ruggedness number ( $R_n$ ), relief ratio ( $R_h$ ), length of overland flow ( $L_g$ ), constant of channel maintenance ( $C$ ), basin relief ( $B_h$ ), hypsometric integral ( $HI$ ), and mean watershed slope ( $P_{mc}$ ). The highest value of linear parameters was assigned to rank one; the second highest value was assigned to rank two and so

**Table 1** Formulas used to determine morphometric parameters

Parameter	Formula	Reference
Stream order ( $U$ )	Hierarchical rank (Strahler scheme)	Strahler (1964)
Stream number ( $N_u$ )	Total no. of stream segments of order “U”	Strahler (1964)
Stream length ( $L_u$ )	The total stream length of order “U” (km)	Horton (1945)
Mean stream length ( $L_{sm}$ )	$L_{sm} = \frac{L_u}{N_u}$	Horton (1945)
Stream length ratio ( $R_l$ )	$R_l = \frac{L_u}{L_{u-1}}$	Horton (1945) Sreedevi et al. (2005)
Bifurcation ratio ( $R_b$ )	$R_b = \frac{N_u}{N_{u+1}}$	Horton (1945) Schumm (1956)
Mean bifurcation ratio ( $R_{bm}$ )	Average of bifurcation ratio of all orders	Strahler (1957, 1964)
Relief ratio ( $R_h$ )	$R_h = \frac{B_h}{L_b}$	Schumm (1956)
Drainage density ( $D$ )	$D = \frac{L_u}{A}$	Horton (1945)
Stream frequency ( $F_s$ )	$F_s = \frac{N_u}{A}$	Horton (1945)
Drainage texture ( $D_t$ )	$D_t = \frac{\sum N_u}{P}$	Horton (1945)
Form factor ( $F_f$ )	$F_f = \frac{A}{L_b^2}$	Horton (1932)
Circulatory ratio ( $R_c$ )	$R_c = \frac{4\pi A}{P^2}$	Miller (1953)
Elongation ratio ( $R_e$ )	$R_e = \frac{2}{L_b} \times \left(\frac{A}{\pi}\right)^{0.5}$	Schumm (1956)
Length of overland flow ( $L_g$ )	$L_g = \frac{1}{2D}$	Schumm (1956)
Constant of channel maintenance ( $C$ )	$C = \frac{1}{D}$	Schumm (1956)
Shape Index ( $S_w$ )	$S_w = \frac{L_u^2}{A}$	Horton (1945)
Ruggedness number ( $R_n$ )	$R_n = B_h \times D$	Strahler (1957)
Compactness coefficient ( $C_c$ )	$C_c = 0.2821 \frac{P}{A^{0.5}}$	Gravelius (1914)
Basin relief ( $B_h$ )	$B_h = H - h$	Schumm (1956)

Where  $L_u$  stream length (km),  $N_u$  stream number (dimensionless),  $L_b$  main channel length (km),  $A$  watershed area (km<sup>2</sup>),  $P$  watershed perimeter (km);  $H$ , maximum elevation of the watershed (m);  $h$ , minimum elevation of the watershed (m)

on. The least value of the linear parameters was given to the last one in the rank. Shape parameters such as elongation ratio ( $R_e$ ), circularity ratio ( $R_c$ ), compactness coefficient ( $C_c$ ), and shape index ( $S_w$ ) have an inverse relationship with erodibility (Biswas et al. 1999; Ratnam et al. 2005; Javed et al. 2009), i.e., the lower the value of the variable is, the greater its influence on degradation degree on watersheds is. Hence, watersheds degradation ranking was determined by assigning priority ranks.

The compound parameter ( $CP$ ), the priority rank ( $NP$ ), and the priority degree ( $GP$ ) of each watershed were also calculated (Patel et al. 2012; Chauhan et al. 2016; Prabhakar et al. 2019).  $CP$  was calculated by averaging all parameters from watersheds. From the group of these watersheds, the highest

priority rank ( $NP$ ) was assigned to the watershed having the lowest compound parameter and so on. The watersheds have been categorized into three classes ( $GP$ ) using the following equations (4, 5, and 6).

$$GP_{High} = \left[ CP_{MIN} , CP_{MIN} + \left( \frac{CP_{MAX} - CP_{MIN}}{3} \right) \right] \tag{4}$$

$$GP_{Medium} = \left[ CP_{MIN} + \left( \frac{CP_{MAX} - CP_{MIN}}{3} \right) , CP_{MIN} + 2 \times \left( \frac{CP_{MAX} - CP_{MIN}}{3} \right) \right] \tag{5}$$

$$GP_{Low} = \left[ CP_{MIN} + 2 \times \left( \frac{CP_{MAX} - CP_{MIN}}{3} \right) , CP_{MAX} \right] \tag{6}$$

In the same way that we calculated the values of  $CP$ ,  $NP$ , and  $GP$  for the component of morphometry, first we calculated the NDVI values, and they were classified following the proposal done by Gómez-Almonte (2005) and Merg et al. (2011). After that, we calculate the  $CP$ ,  $NP$ , and  $GP$  as suggested by Patel et al. (2012), Chauhan et al. (2016), and Prabhakar et al. (2019). The  $GP$  values were calculated applying Equations (4), (5), and (6), and classified as a function of high, medium, and low ranks.

**Table 2** Classification of NDVI values

Rating	NDVI value
Bare soil	0.01–0.10
Low cover	0.10–0.20
Medium cover	0.2–0.40
High cover	> 0.40

## Results and discussion

### Main sub-basin characteristics

The parameters of shape, relief, and those relative to drainage network were calculated and presented in Table 3. The results indicate that in the upper part of the sub-basin, the water flow runs at high velocities generating a torrential flow. In the lower part, there are peak flows caused by surface runoff concentration. The sub-basin time of concentration is 3.37 h along 41.59 km of the main channel and reaches flows with highly erosive velocities. The sub-basin is elongated, classified as order seven. The sub-basin presents high drainage density and outstanding stream frequency. The sub-basins' drainage system is dendritic and presents a mean bifurcation ratio around four streams before discharging into a stream of higher order.

The sub-basin's mean terrain slope is 38.79%, and the main channel's mean slope is 6.4%; gradients greater than 100% are found in its upper area, and they influence directly erosive processes. Based on the longitudinal profile of the main channel, the sub-basin's upper sector is approximately 2700 m above mean sea level, and the slope of the first 10 km downstream of the main channel is greater than 100%. Following the course downstream, between 10 and 20 km approximately along the main

channel, the slope decreases. In the last part of the main channel (from 28 to 42 km), i.e., downstream, the slope is less than 10%. Due to these variations, the main channel's mean slope is 6.4%; yet we must consider the slope variations along the main channel linked to the changes in length and elevation (Fig 3). The sub-basin's mean terrain slope and the main channel's mean slope values are important since they define the potential runoff and have a strong correlation with soil erosion, particles detachment on streams, sediments transport capacity, and volume of sediment deposited in the lower parts of the sub-basin. The sediments deposited in the lower parts of the sub-basin cause that the main channels lose part of their hydraulic section making agricultural and urban areas more prone to flooding.

The sub-basin's hypsometric-adjusted curve corresponds to a third-degree polynomial model, and its integration produces an area of 30.47% below the curve and which according to Strahler (1952, 1957) corresponds to a sub-basin at an old stage (monadnock phase). According to the sub-basin's morphometry and geofoms, relative areas at the beginning of the hypsometric curve present strong erosive processes caused by high runoff velocities and which are attenuated downward creating accumulation zones from transported materials (Fig 4).

### Morphometric parameters of watersheds

Drainage analysis coupled with hydrological observations provides useful information about the geological framework of the basin. The main factors controlling the evolution of the basin are rainfall availability as the source of water, drainage characteristics and its influence on runoff and infiltration capacity, rock type for which the lithology character governs the movement of the water, and slope because it controls the water energy flow. These factors can define variations between morphometric parameters and can be measure it by GIS (Singh et al. 2014).

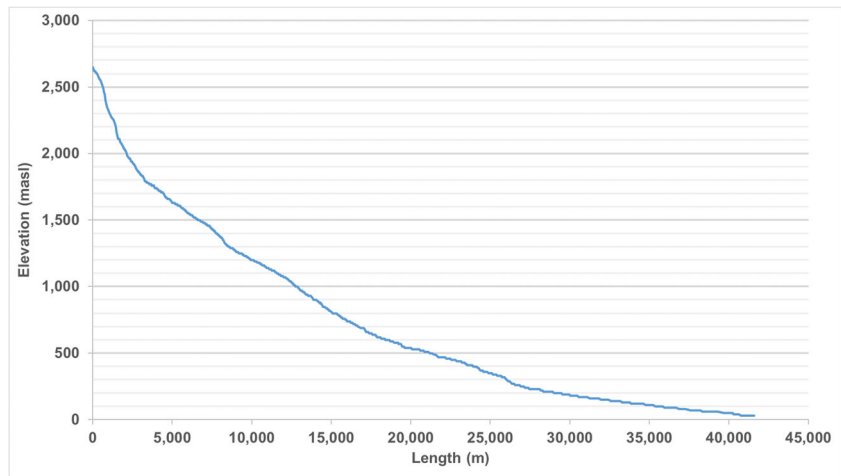
On each delineated watershed, the morphometric parameters, geofoms, and soil physical properties vary according to their topography, for example, the slope is higher upstream. In relation to the area, the largest corresponds to watershed 01, followed by watershed 08, located at the lower and upper sectors of the sub-basin, respectively (Table 4). The mean slopes of each watershed increase according to its mean elevations, being the watersheds 07 and 08 (located in the sub-basin upper part) the steepest ones.

The  $P_{mc}$  values, in relation to  $P_{Ic}$ , are close to or greater than 20% in all watersheds, being the smallest difference on watershed 02, with 19.58%, and the largest on watershed 07, with 51.83%. These differences in slope, between terrain and channel, are related to topographic relief, drainage network density, and shape of channel cross-sections.

**Table 3** Morphometric parameters determined for Huehuetan river sub-basin

Morphometric parameter	Value
Area (km <sup>2</sup> )	319.41
Perimeter (km)	132.68
Main channel length (km)	41.59
Shape index (dimensionless)	0.185
Circularity ratio (dimensionless)	0.23
Compactness coefficient (dimensionless)	2.09
Elongation ratio (dimensionless)	0.48
Mean terrain slope (%)	38.79
Main channel slope (%)	6.40
Drainage system	Dendritic
Drainage type	Dendritic
Time of concentration (hour)	3.37
Drainage density (km/km <sup>2</sup> )	5.03
Stream frequency (streams/km <sup>2</sup> )	19.96
Total stream length (km)	1607.24
Order number (dimensionless)	7
Minimum elevation (masl)	30
Mean elevation (masl)	858.13
Maximum elevation (masl)	2690
Mean bifurcation ratio (dimensionless)	4.02

**Fig. 3** Longitudinal profile of the main channel for the Huehuetan river sub-basin



**Stream order (*U*)**

The stream order (*U*) is a morphometric parameter that determines the stream hierarchy of tributaries, and the higher the stream order is, the larger discharges and erosive velocities are (Mahala 2020). In the Huehuetan river sub-basin, the stream orders are six (watersheds 01, 04, 06, and 08), five (watersheds 03 and 07), and four (watersheds 02 and 05). In our case, the stream number decreases as the order number increases, and this can be explained by Horton’s law of streams (Horton 1945). In Figure 5, we present a graph that shows our data following a linear trend when graphing the stream order relative to the logarithms of the stream number. Any variation in this figure is related to changes in geological structures, active tectonics (Kamberis et al. 2012), lithology (Singh et al. 2014), and consequently, in relief and slope terrain and channels.

**Stream length (*L<sub>u</sub>*)**

The stream length (*L<sub>u</sub>*) is a hydrological feature affected by the slope. The higher slope is, the higher erosive velocities are, generating a dense stream network on upper lands but shorter on length (first order). However, when all streams are accumulated, it produces a larger total stream length (*L<sub>u</sub>*). In contrast, smaller slopes will influence the stream order with less dense by increasing channel length and the total length to be shorter (Gopinath et al. 2016). In general, the sum of stream length decreases as the order number increases (Ramaiah et al. 2012; Magesh et al. 2013) and which is consistent with Horton’s law of streams (Horton 1945). Our results indicate that eight watersheds (Fig 6) fit Horton’s laws although some of them showed an inverse relationship mainly on the 3rd and 4th order (watersheds 01, 02, 07), due to their physical conditions that increase the drainage network to higher orders. Besides topography, lithology (Mishra and Nagarajan 2010),

**Fig. 4** The hypsometric curve obtained and adjusted for the Huehuetan river sub-basin

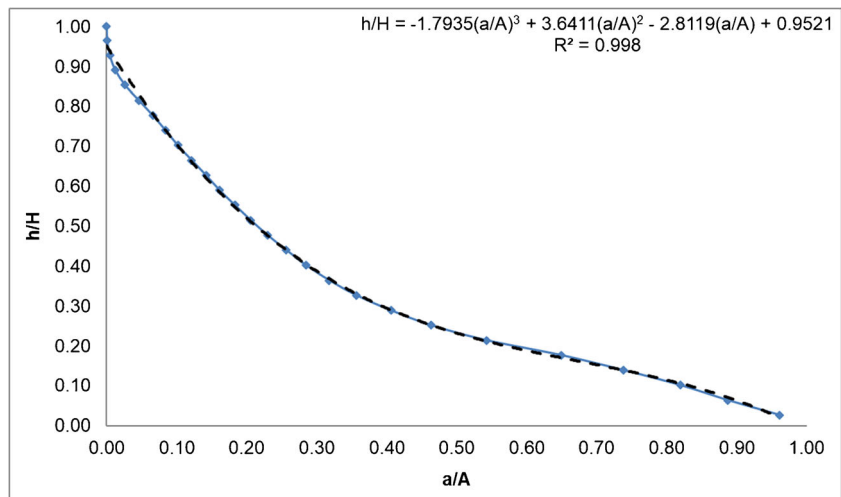


**Table 4** Watersheds morphometric parameters for the Huehuetan river sub-basin

Watershed	A (km <sup>2</sup> )	P (km)	L <sub>c</sub> (km)	L <sub>tc</sub> (km)	P <sub>lc</sub> (%)	P <sub>mnc</sub> (%)	Elevation (masl)			B <sub>h</sub> (m)	N <sub>u</sub>	T <sub>c</sub> (h)	U
							Min.	Max.	Mean				
1	129.50	97.72	40.96	618.74	4.71	25.75	30.00	1960.00	469.00	1930.00	1495.00	3.75	VI
2	25.52	53.18	16.79	99.93	3.75	23.33	30.00	660.00	246.00	630.00	196.00	2.06	IV
3	41.59	48.02	19.41	215.15	11.42	41.42	213.00	2430.00	903.00	2217.00	505.00	1.50	V
4	16.57	26.78	9.57	83.94	6.69	32.87	210.00	850.00	529.00	640.00	192.00	1.07	VI
5	14.23	26.52	10.02	76.02	20.06	57.67	510.00	2520.00	1205.00	2010.00	179.00	0.73	IV
6	14.25	32.20	10.94	83.28	19.38	43.07	510.00	2630.00	960.00	2120.00	207.00	0.79	VI
7	25.92	37.48	13.23	145.28	15.12	66.95	660.00	2660.00	1745.00	2000.00	415.00	1.00	V
8	51.70	47.20	18.03	279.75	11.26	58.12	660.00	2690.00	1651.00	2030.00	738.00	1.42	VI
<b>Max.</b>	129.50	97.72	40.96	618.74	20.06	66.95	660.00	2690.00	1745.00	2217.00	1495.00	3.75	VI
<b>Min.</b>	14.23	26.52	9.57	76.02	3.75	23.33	30.00	660.00	246.00	630.00	179.00	0.73	IV
<b>Mean</b>	39.91	46.14	17.37	200.26	11.55	43.65	352.90	2050.00	963.50	1697.13	499.00	1.54	--
σ	38.61	23.13	10.25	184.16	6.30	16.05	263.60	833.60	546.88	661.17	451.90	0.99	--
<b>CV (%)</b>	96.74	50.12	58.99	91.96	54.55	36.78	74.70	40.70	56.76	38.96	92.10	64.48	--

Where A watershed area, P perimeter, L<sub>c</sub> length of main channel, L<sub>tc</sub> total stream length, P<sub>lc</sub> main channel slope, P<sub>mnc</sub> mean watershed slope, B<sub>h</sub> watershed relief, N<sub>u</sub> total number of streams, T<sub>c</sub> time of concentration, U stream order, Max, Min., and Mean maximum, minimum, and average values, respectively, σ standard deviation, CV variation coefficient

and tectonic processes, there are physical conditions that affect expected line trends in the drainage area (Migiro et al. 2011; Kamberis et al. 2012; Hajam et al. 2013).

On the other hand, the mean stream length (L<sub>sm</sub>) is directly proportional to the stream order (U) and follows a geometric progression (Table 5) as suggested by Horton’s law of streams (Horton 1945). The stream length ratio (R<sub>l</sub>) also follows this behavior, although in some watersheds the values decrease, as observed from the relationship between 4th and 5th orders. This unexpected behavior is associated with tectonic processes (Kamberis et al. 2012) and its lithological responses that

have occurred in the drainage areas and have generated changes on relief and slopes in some sectors of the sub-basin (Strahler 1957; Phani 2014; Gopinath et al. 2016).

**Bifurcation ratio (R<sub>b</sub>)**

The bifurcation ratio (R<sub>b</sub>) expresses the relationship between the stream number from a given order and the stream number on the next lower order (Schumm 1956). The variation in this parameter in the same watershed is related to local geological conditions that affect lithological characteristics, drainage

**Fig. 5** Relationship between stream order and stream number, by watershed, in the Huehuetan river sub-basin

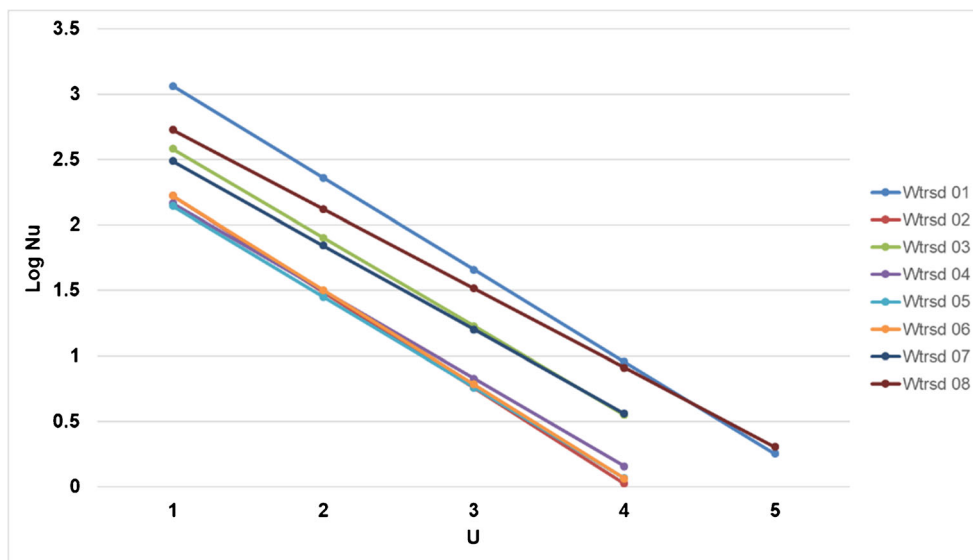
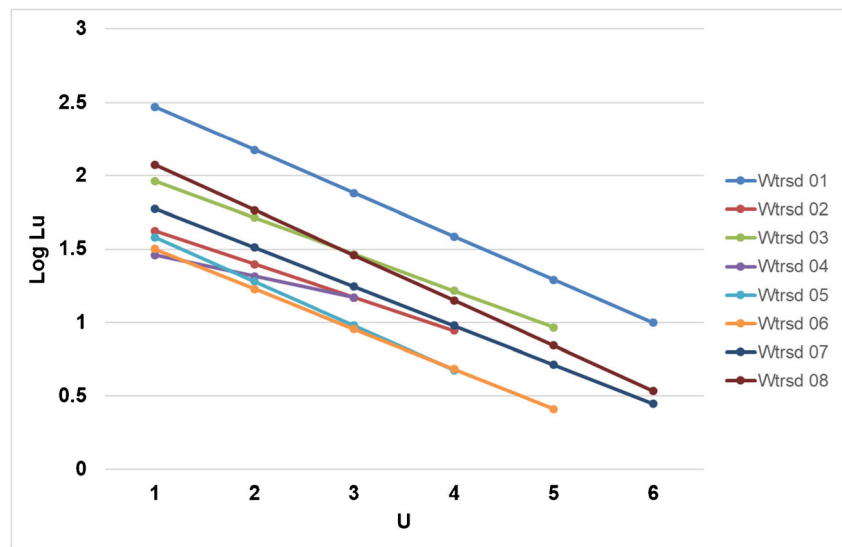




**Fig. 6** Relationship between stream order and stream length, by watershed, in the Huehuetan river sub-basin



density, angle of connection between channels, and watershed shape and size (Singh and Dubey 2012). In our study, the Huehuetan river sub-basin presents high values of  $R_b$  between 7.0 and 2.0 while the mean ratios by watershed between 5.46 and 3.71. These high  $R_b$  values are related to early hydrograph peaks, potential for flash floods (Howard 1990; Rakesh et al. 2000), soil erosion susceptibility, and gully formation, processes affected by geological and lithological evolution such as deformation patterns, tectonism, and mass movements (Kamberis et al. 2012).

**Drainage density**

The drainage density ( $D$ ) is a parameter related to the total stream length and watershed area (Horton 1945); it varies with

the rainfall intensity, rock permeability, soil infiltration, and watershed slope. The magnitude of the drainage density controls landforms, soil erosion, and vegetation cover (Horton 1932; Strahler 1964) and provides a numerical measurement for landscape dissection, drainage efficiency, and runoff potential (Magesh et al. 2013). For the Huehuetan river sub-basin, the extreme  $D$  values vary from 3.92 to 5.78 km/km<sup>2</sup> for watersheds 02 and 06, respectively (Table 6). In our study, while high values are associated with high topographic relief, impermeable rocks, superficial soils, and scarce vegetation cover, low values are linked to watersheds with permeable subsurface material, good vegetation cover, and low relief that increase the infiltration capacity. Singh and Singh (2011) and Singh et al. (2014) found similar results for other watersheds.

**Table 5** Stream length and stream length ratio, by watershed and stream order, on the Huehuetan sub-basin

Watershed	Mean stream length ( $L_{sm}$ , km)						Stream length ratio ( $R_i$ )				
	1st	2nd	3rd	4th	5th	6th	2nd/1st	3rd/2nd	4th/3rd	5th/4th	6th/5th
1	0.295	0.490	1.365	7.620	9.415	9.070	1.661	2.784	5.583	1.236	0.963
2	0.372	0.581	1.750	11.830	--	--	1.560	3.014	6.760	--	--
3	0.305	0.445	2.169	3.413	11.430	--	1.456	4.878	1.573	3.349	--
4	0.345	0.516	1.223	6.200	--	--	1.494	2.370	5.070	--	--
5	0.320	0.465	2.107	4.570	--	--	1.452	4.534	2.169	--	--
6	0.323	0.466	1.233	2.135	0.900	--	1.442	2.648	1.732	0.422	--
7	0.281	0.374	0.676	2.918	6.410	--	1.330	1.807	4.313	2.197	--
8	0.312	0.410	0.809	1.659	1.125	9.000	1.313	1.974	2.051	0.678	8.000
<b>Mean</b>	<b>0.319</b>	<b>0.468</b>	<b>1.417</b>	<b>5.043</b>	<b>5.856</b>	<b>9.035</b>	<b>1.464</b>	<b>3.001</b>	<b>3.656</b>	<b>1.576</b>	<b>4.482</b>

**Table 6** Morphometric parameters for each watershed

Watershed	<i>A</i>	<i>D</i>	<i>F<sub>s</sub></i>	<i>D<sub>t</sub></i>	<i>F<sub>f</sub></i>	<i>R<sub>e</sub></i>	<i>R<sub>c</sub></i>	<i>R<sub>bm</sub></i>	<i>R<sub>n</sub></i>	<i>R<sub>h</sub></i>	<i>L<sub>g</sub></i>	<i>C</i>	<i>C<sub>c</sub></i>	<i>B<sub>h</sub></i>	<i>HI</i>	<i>P<sub>mc</sub></i>	<i>S<sub>w</sub></i>
1	129.50	4.78	11.53	15.29	0.08	0.31	0.17	4.40	9.22	0.05	0.10	0.21	2.42	1930.00	0.22	0.26	12.95
2	25.52	3.92	7.73	3.70	0.09	0.34	0.11	5.42	2.47	0.04	0.13	0.26	2.97	630.00	0.35	0.23	11.06
3	41.59	5.17	12.14	10.52	0.11	0.37	0.23	4.57	11.47	0.11	0.10	0.19	2.10	2217.00	0.31	0.41	9.06
4	16.57	4.64	11.53	7.13	0.18	0.48	0.29	5.46	2.97	0.07	0.11	0.22	1.86	640.00	0.50	0.33	5.53
5	14.23	5.34	12.58	6.75	0.14	0.42	0.25	5.32	10.74	0.20	0.09	0.19	1.98	2010.00	0.35	0.58	7.06
6	14.25	5.78	14.74	6.52	0.12	0.39	0.17	3.81	12.25	0.19	0.09	0.17	2.41	2120.00	0.22	0.43	8.40
7	25.92	5.61	16.01	11.07	0.15	0.43	0.23	4.30	11.21	0.15	0.09	0.18	2.08	2000.00	0.54	0.67	6.75
8	51.70	5.41	14.27	15.64	0.16	0.45	0.29	3.71	10.98	0.11	0.09	0.18	1.85	2030.00	0.49	0.58	6.29
<b>Max.</b>	<b>129.50</b>	<b>5.78</b>	<b>16.01</b>	<b>15.64</b>	<b>0.18</b>	<b>0.48</b>	<b>0.29</b>	<b>5.46</b>	<b>12.25</b>	<b>0.20</b>	<b>0.13</b>	<b>0.26</b>	<b>2.97</b>	<b>2217.00</b>	<b>0.54</b>	<b>0.67</b>	<b>12.95</b>
<b>Min.</b>	<b>14.23</b>	<b>3.92</b>	<b>7.73</b>	<b>3.70</b>	<b>0.08</b>	<b>0.31</b>	<b>0.11</b>	<b>3.71</b>	<b>2.47</b>	<b>0.04</b>	<b>0.09</b>	<b>0.17</b>	<b>1.85</b>	<b>630.00</b>	<b>0.22</b>	<b>0.23</b>	<b>5.53</b>
<b>Mean</b>	<b>39.91</b>	<b>5.08</b>	<b>12.57</b>	<b>9.58</b>	<b>0.13</b>	<b>0.40</b>	<b>0.22</b>	<b>4.62</b>	<b>8.91</b>	<b>0.12</b>	<b>0.10</b>	<b>0.20</b>	<b>2.21</b>	<b>1697.13</b>	<b>0.37</b>	<b>0.44</b>	<b>8.39</b>
$\sigma$	<b>38.61</b>	<b>0.61</b>	<b>2.54</b>	<b>4.32</b>	<b>0.03</b>	<b>0.06</b>	<b>0.06</b>	<b>0.70</b>	<b>3.92</b>	<b>0.06</b>	<b>0.01</b>	<b>0.03</b>	<b>0.38</b>	<b>661.17</b>	<b>0.13</b>	<b>0.16</b>	<b>2.55</b>
<b>CV (%)</b>	<b>96.74</b>	<b>11.96</b>	<b>20.22</b>	<b>45.06</b>	<b>27.05</b>	<b>14.34</b>	<b>29.05</b>	<b>15.23</b>	<b>43.96</b>	<b>53.00</b>	<b>14.14</b>	<b>14.64</b>	<b>17.08</b>	<b>38.96</b>	<b>33.94</b>	<b>36.78</b>	<b>30.37</b>

Where *A* watershed area (km<sup>2</sup>), *D* drainage density (km/km<sup>2</sup>), *F<sub>s</sub>* stream frequency (streams/km<sup>2</sup>), *D<sub>t</sub>* drainage texture (dimensionless), *F<sub>f</sub>* form factor (dimensionless), *R<sub>e</sub>* elongation ratio (dimensionless), *R<sub>c</sub>* circularity ratio (dimensionless), *R<sub>bm</sub>* mean bifurcation ratio (dimensionless), *R<sub>n</sub>* ruggedness number (dimensionless), *R<sub>h</sub>* relief ratio (dimensionless), *L<sub>g</sub>* length of overland flow (km), *C* constant of channel maintenance (km<sup>2</sup>/km), *C<sub>c</sub>* compactness coefficient (dimensionless), *B<sub>h</sub>* basin relief (m), *HI* hypsometric integral (%), *P<sub>mc</sub>* watershed mean slope (%), *S<sub>w</sub>* shape index (dimensionless)

### Stream frequency

According to Horton (1945), stream frequency (*F<sub>s</sub>*) is the ratio between the total number of reach segments for all stream orders and the watershed area. Hypothetically, it is possible to have watersheds with the same drainage density but differs in stream frequency and vice versa (Ramaiah et al. 2012). The stream frequency is associated with the evolution of the landscape (Magesh et al. 2013); it mainly depends on the watershed lithology and it influences the drainage texture (Hajam et al. 2013). Low *F<sub>s</sub>* values are related to high permeable lithology (Joji et al. 2013; Abboud and Nofal 2017) and low flood occurrence (Maurya et al. 2016). However, areas of permeable soils exposed to intense rainfall events and high frequency can produce runoff due to soil saturation or insufficient infiltration capacity which, at the same time, cause the creation of new streams and trigger landslides. Our results indicate that higher *F<sub>s</sub>* values are in the upper part of the sub-basin, mainly in watersheds 07, 06, and 08, indicating soils susceptible to erosion and gully formation. In addition, *F<sub>s</sub>* is directly proportional to drainage density.

### Drainage texture

The drainage texture (*D<sub>t</sub>*) is a parameter corresponds to the relationship between the total number of streams for all stream orders and the perimeter of the watershed. According to Horton (1945), *D<sub>t</sub>* represents the relative spacing among drainage lines and depends mainly on infiltration capacity, although it is also affected in a lower degree by rainfall,

vegetation cover, and rocks permeability (Dash et al. 2013). Smith (1950) classified the drainage texture in five classes: very coarse (<2), coarse (2–4), moderate (4–6), fine (6–8), and very fine (>8). Based on this classification, the sub-basin textures of our study (Table 6) fall into the categories of coarse texture (watershed 02), fine (watersheds 06, 05, and 04), and very fine (watersheds 01 and 08). The variation of *D<sub>t</sub>* values for our study indicates a high drainage network dissection and potential for runoff.

### Form factor

According to Horton (1932), the form factor (*F<sub>f</sub>*) parameter correlates the watershed area and the square of the watershed's channel length. The *F<sub>f</sub>* parameter is also an indicator of watershed topographic relief, geological structures, and erosivity of the channel's bed material (Abboud and Nofal 2017). Watersheds with high form factors have a circular shape and big peak flows but short time of concentration, whereas elongated watersheds with low form factors have low peak flows and large time of concentration (Altaf et al. 2013; Kumar and Chaudhary 2016; Kusre 2016). In this study, all watersheds have a low form factor (*F<sub>f</sub>*<0.20) and fitting the elongated shape of the watersheds and capable to manage floods better than those watersheds with circular forms.

### Shape index

The shape index (*S<sub>w</sub>*) is reciprocal to the form factor (*F<sub>f</sub>*) and relates the stream length and watershed area. This index is

associated with topographic relief, sediment transport, and flow concentration time (Vincy et al. 2012; Altaf et al. 2013). The values of the shape index for the studied watersheds varied from 5.53 in watershed 04 to 12.95 in watershed 01 (refer to Table 6). Those  $S_w$  values suggest that watershed 04 has the shortest concentration time, while the watershed 01 will have the longest concentration time.

### Elongation ratio

The elongation ratio ( $R_c$ ) relates the diameter of a circle, with an area similar to the watershed, and the maximum stream length (Schumm 1956).  $R_c$  compares the watershed shape to a circle, and its magnitude depends on the climatic and geologic past conditions of the sub-basin (Rai et al. 2017). The elongation ratio, proposed by Schumm (1956) and further interpreted by Strahler (1964), is used to evaluate the shape of the watersheds, i.e., circular (0.9–1.0), oval (0.8–0.9), less elongated (0.7–0.8), elongated (0.5–0.7), and more elongated (< 0.5) (Gupta et al. 2019). Elongated watersheds indicate a young stage of evolution caused by intense neotectonic activities, while a watershed with a shape close to a circle suggests an early stage of maturity (Lykoudi and Angelaki 2004). A circular watershed is more efficient to discharge runoff than an elongated one (Singh and Singh 1997). The  $R_c$  values for the watersheds of our study varied between 0.31–0.48, and they can be classified as more elongated. The  $R_c$  values of the watersheds help to explain the neotectonic influence on basin's evolution, and high speed flows on channels (Strahler 1952).

### Circularity ratio

The circularity ratio ( $R_c$ ) is a quantitative parameter that allows visualizing the shape of the watershed. The  $R_c$  relates the area of a watershed to the area of a circle with a circumference that is equal to the perimeter of the watershed, i.e., both the watershed and the circle must have the same perimeter, but the area can vary (Miller 1953; Strahler 1964). The  $R_c$  parameter is affected by geological structures, vegetation cover, climate, relief, and slope (Vincy et al. 2012; Aher et al. 2014) and is used to correlate stream frequency, watershed shape, and runoff (Al-Saady et al. 2016). Magesh et al. (2011) reported that the  $R_c$  is related to the age of the watershed and it can be classified as low, medium, and high indicating that a watershed can be at youth, mature, and old stages of the life cycle, respectively.

### Length of overland flow

The length of the overland flow ( $L_g$ ) comprises the water that flows over the ground surface to stream channels. The overland flow occurs due to the inability of water to infiltrate the

ground surface, either because of the high intensity of rainfall or because of soil poor infiltration capacity (Horton 1945; Schumm 1956). Horton (1945) defines  $L_g$  as the half of the reciprocal value of the drainage's density ( $D$ ) and it depends on channel slope and current vegetation cover conditions (Aher et al. 2014).  $L_g$  holds an inverse relationship with channel mean slope, and it is similar to the laminar flow length (Magesh et al. 2011); hence, the slope is important for the hydrological response of watersheds (Aher et al. 2014). The  $L_g$  values in our work varied from 0.09 to 0.13 km, indicating that the overland flow moves over short distances before runoff concentrates into tributary channels; this situation is mainly due to steep slope conditions, scarce vegetation, and soil susceptibility to generate gullies; causing the high values of drainage density and stream frequency.

### Constant of channel maintenance

Schumm (1956) used the reciprocal of drainage density to represent the area needed to maintain 1 km of channel and called constant of channel maintenance ( $C$ ). This parameter depends on rock type, permeability, vegetation cover, and topographic relief (Kouli et al. 2007; Dash et al. 2013), and it is an indicator of watershed erodibility (Singh and Singh 2011). The results in Table 6 show low values because the watersheds in our study have scarce vegetation, soils with low resistance to runoff, and mountainous relief (Altaf et al. 2013).

### Compactness coefficient

The compactness coefficient ( $C_c$ ), also known as Gravelius Index (GI), divides the watershed perimeter by a circumference with a similar area to this one. During rainfall events,  $C_c$  influences the amount of runoff and the shape of the hydrograph (Graveluis 1914; Maurya et al. 2016). From the hydrological standpoint, circular watersheds produce the most hazardous conditions because they produce, for similar surfaces, the shortest time of concentration and the highest peak flow (Ratnam et al. 2005; Javed et al. 2009; Altaf et al. 2013; Chandniha and Kansal 2017). When watershed tends to be circular, the relative distance from any point at the perimeter of the basin to the main channel is practically the same, and the concentration time becomes lower causing greater accumulation of surface runoff, bigger erosive velocities, and larger floods along the main channel. A  $C_c$  value equal to one occurs when the watershed shape is a perfect circle; a factor of 1.128 corresponds to a square-shaped watershed, and a coefficient around 3.00 is related to very elongated watersheds (Al-Saady et al. 2016). Based on our results (Table 6), the watersheds show square-shaped and very elongated shapes.

### Ruggedness number

The ruggedness number ( $R_n$ ) parameter is the relation between the watershed topographic relief and the drainage density (Strahler 1957); it combines the slope-length characteristics in one expression. Areas with low watershed topographic relief but high drainage density are ruggedly textured, and areas of higher topographic relief have lower dissection.  $R_n$  indicates that if the drainage density increases while the relief remains constant, the average horizontal distance from drainage divide to the contiguous channel will be reduced. On the other hand, if the drainage density remains constant and the watershed topographic relief increases, the elevation difference will increase (Aher et al. 2014). The  $R_n$  values calculated for our study (Table 6) show that the Huehuetan watersheds exhibit steep slopes, high relief, and high drainage density.

### Relief ratio

The relief ratio ( $R_h$ ) is the relationship between the total relief of a watershed and the longest horizontal distance measured along its main channel (Schumm 1956).  $R_h$  measures the overall watershed steepness, and it is directly related to the length of overland flow and time for peak flood (Singh et al. 2014). Thus,  $R_h$  is an important indicator for general erosion and intensity (Samal et al. 2015). High values of  $R_h$  indicate a steep slope and high relief, while a lower slope value may be controlled by basement rocks in form of small ridges and mounds (Vitala et al. 2004). The  $R_h$  values (Table 6) obtained in our study are directly related to watershed topographic relief conditions, in the sub-basin, upper part are steeper slopes and higher  $R_h$  values (i.e., watersheds 05 and 06), while the lowest value (0.04) was found in the watershed 02. Our results align with the findings of Ansari et al. (2012), Joji et al. (2013), Aher et al. (2014), Babu et al. (2016), Kumar and Chaudhary (2016), and Abboud and Nofal (2017); they report similar behaviors of the  $R_h$  values for other watersheds.

### Hypsometric integral

The hypsometric integral (HI) of a watershed represents the relative area under a given altitude (Strahler 1952). The hypsometric curve (HC) presents on the ordinate axis; the watershed elevation in relation to its maximum altitude, and on the abscissae axis, presents the relative areas with respect to the watershed surface. The relative values (percentages) presented in the curve allow comparisons between curves from different watersheds (Racca 2007). The hypsometric curves of a watershed are associated with flood responses, watershed erosion, and drainage network development and allow to identify active and inactive tectonic sectors (Al-Saady et al. 2016).

The value of the hypsometric integral, expressed in percentage, compares a given volume at time “ $t$ ” in the watershed

and its initial value, allowing to estimate the erosion volume occurred on the watershed along its geological span time (Bishop et al. 2002). Strahler (1952) found that HI has an inverse relationship with watershed relief, slope length, drainage density, and channel slope.

The hypsometric curve and the hypsometric integral can be associated with the watershed dissection degree and the relative age of its topographic relief. The convex curves in the upper part with high values of the hypsometric integral ( $HI > 60\%$ ) are linked to early youth watersheds with little degraded landscapes but intense erosion processes (youth or inequilibrium stage). The S-shaped curves indicate that watersheds are close to full maturity ( $35\% < HI < 60\%$ ) and landscapes are close to equilibrium stage and lower degradation processes. The concave curves, with low HI values ( $< 35\%$ ), are typical on dissected landscapes and old watersheds where degradation processes are minimal (monadnock stage) (Strahler 1952).

### Correlation matrix between morphometric parameters

The correlation between morphometric parameters using the Pearson correlation coefficient ( $r$ ) are summarized in Table 7. The results indicate that 20 values were highly positive correlations (with greater than 0.70). These correlations were watershed area ( $A$ ) with drainage texture ( $D_t$ ), drainage density ( $D$ ) with stream frequency ( $F_s$ ), ruggedness number ( $R_n$ ), relief ratio ( $R_h$ ), basin relief ( $B_h$ ), and mean watershed slope ( $P_{mc}$ ); stream frequency ( $F_s$ ) with ruggedness number ( $R_n$ ), basin relief ( $B_h$ ), and mean watershed slope ( $P_{mc}$ ); form factor ( $F_f$ ) with elongation ratio ( $R_e$ ), circularity ratio ( $R_c$ ), and hypsometric integral (HI); elongation ratio ( $R_e$ ) with circularity ratio ( $R_c$ ), and hypsometric integral (HI); mean bifurcation ratio ( $R_{bm}$ ) with constant of channel maintenance ( $C$ ); ruggedness number ( $R_n$ ) with relief ratio ( $R_h$ ) and basin relief ( $B_h$ ); length of overland flow ( $L_g$ ) with constant of channel maintenance ( $C$ ); and compactness coefficient ( $C_c$ ) with shape index ( $S_w$ ).

On the other hand, we found 22 negative correlations with high level of significance, i.e., the mean bifurcation ratio ( $R_{bm}$ ) with stream frequency ( $F_s$ ); ruggedness number ( $R_n$ ) with mean bifurcation ratio ( $R_{bm}$ ); both length of overland flow ( $L_g$ ) and constant of channel maintenance ( $C$ ) with drainage density ( $D$ ), stream frequency ( $F_s$ ), ruggedness number ( $R_n$ ), and relief ratio ( $R_h$ ); compactness coefficient ( $C_c$ ) and shape index ( $S_w$ ) with form factor ( $F_f$ ), elongation ratio ( $R_e$ ), and circularity ratio ( $R_c$ ); basin relief ( $B_h$ ) with mean bifurcation ratio ( $R_{bm}$ ), length of overland flow ( $L_g$ ), and constant of channel maintenance ( $C$ ); and mean watershed slope ( $P_{mc}$ ) with length of overland flow ( $L_g$ ), and constant of channel maintenance ( $C$ ). We also found 16 comparisons did not correlate (values between  $-0.10 < r < 0.10$ ), i.e., watershed area

**Table 7** Correlation coefficients of the morphometric parameters

A	D	F <sub>s</sub>	D <sub>t</sub>	F <sub>r</sub>	R <sub>c</sub>	R <sub>hm</sub>	R <sub>n</sub>	R <sub>h</sub>	L <sub>g</sub>	C	C <sub>c</sub>	B <sub>h</sub>	HI	P <sub>mc</sub>	S <sub>w</sub>
A	1.000														
D	-0.170	1.000													
F <sub>s</sub>	-0.122	0.948**													
D <sub>t</sub>	0.735*	0.337	1.000												
F <sub>r</sub>	-0.535	0.363	0.435	1.000											
R <sub>c</sub>	-0.596	0.367	0.472	0.996**	1.000										
R <sub>c</sub>	-0.194	0.424	0.491	0.862**	0.841**	1.000									
R <sub>hm</sub>	-0.286	-0.698	-0.710*	0.637	0.020	0.027	-0.077	1.000							
R <sub>n</sub>	0.116	0.896**	0.784*	-0.014	-0.011	0.207	-0.744*	1.000							
R <sub>h</sub>	-0.507	0.838**	0.696	0.320	0.355	0.263	-0.303	0.714*	1.000						
L <sub>g</sub>	-0.034	-0.954**	-0.909**	-0.348	-0.336	-0.512	0.657	-0.897**	1.000						
C	0.078	-0.989**	-0.932**	-0.435	-0.350	-0.479	0.727*	-0.777*	0.966**	1.000					
C <sub>c</sub>	0.139	-0.566	-0.613	-0.426	-0.780*	-0.978**	0.172	-0.370	0.656	0.620	1.000				
B <sub>h</sub>	0.238	0.828*	0.708*	0.549	-0.111	0.176	-0.718*	0.988**	-0.860**	-0.860**	-0.341	1.000			
HI	-0.376	0.057	0.283	0.112	0.798*	0.643	0.109	-0.204	-0.050	-0.035	-0.542	-0.265	1.000		
P <sub>mc</sub>	-0.360	0.789*	0.816*	0.260	0.578	0.570	-0.399	0.741*	-0.774*	-0.751*	-0.632	0.589	0.526	1.000	
S <sub>w</sub>	0.683	-0.466	-0.534	0.085	-0.967**	-0.816*	0.015	-0.488	0.405	0.440	0.772*	-0.002	-0.743*	-0.677	1.000

Where A watershed area (km<sup>2</sup>), D drainage density (km/km<sup>2</sup>), F<sub>s</sub> stream frequency (streams/km<sup>2</sup>), D<sub>t</sub> drainage texture (dimensionless), F<sub>r</sub> form factor (dimensionless), R<sub>c</sub> elongation ratio (dimensionless), R<sub>c</sub> circularity ratio (dimensionless), R<sub>hm</sub> mean bifurcation ratio (dimensionless), R<sub>n</sub> ruggedness number (dimensionless), R<sub>h</sub> relief ratio (dimensionless), L<sub>g</sub> length of overland flow (km), C constant of channel maintenance (km<sup>2</sup>/km), C<sub>c</sub> compactness coefficient (dimensionless), B<sub>h</sub> basin relief (m), HI hypsometric integral (%), P<sub>mc</sub> watershed mean slope (%), S<sub>w</sub> shape index (dimensionless). Significance level

\* p<0.05

\*\* p<0.01

(A) with length of overland flow ( $L_g$ ) and drainage density ( $D$ ) with hypsometric integral (HI).

The correlation analysis shows a high level of correspondence ( $p < 0.01$ ) among 17 variables compared. Drainage density ( $D$ ), length of overland flow ( $L_g$ ), and constant of channel maintenance ( $C$ ) were the most associated variables with five correlations, followed by compactness coefficient ( $C_c$ ) and shape index ( $S_w$ ) with four correlations each one, while stream frequency ( $F_s$ ), form factor ( $F_f$ ), ruggedness number ( $R_n$ ), and basin relief ( $B_h$ ) shown three significant correlations each one. On the other hand, watershed area ( $A$ ) and relief ratio ( $R_h$ ) were associated ( $p < 0.05$ ) only with drainage texture ( $D_t$ ) and mean watershed slope ( $P_{mc}$ ), respectively. We identified that the main correlations are related to five linear morphometric parameters and the correlation with four of these parameters are associated with shape parameters, and correlations with three parameters correspond to relief. Despite these correlations allow identifying high and significant relationship among parameters, they do not allow yet to group specific parameters into components and try to attach any physical significance (Sharma et al. 2015). Thus, the resulting large number data from the correlation analysis justifies the need for a procedure to discriminate parameters and find those parameters that have greater influence on basin's evolution and its degradation without losing quality of the explanation of each selected variable.

Due to a large number of correlations among morphometric parameters, we used the principal component analysis to determine which morphometric parameters have greater influence on watersheds behavior. Multivariate analysis is a useful technique for identifying common patterns in data distribution, leading to a reduction of the initial dimension of datasets and facilitating their interpretation (Khanchoul and Saaidia 2017).

### Principal component analysis

We applied the principal component analysis (PCA) technique to all morphometric parameters that have influence on soil degradation process in the eight watersheds of the Huehuetan river sub-basin (Table 8). PCA is based on a

“component loading” matrix and indicates numerically the level of relationship between each component and the original morphometric parameters (Farhan et al. 2017). The weights of the original parameters in each component are called “loadings,” and each component is associated with a particular parameter. Besides interpreting the processes that generate the observed relationships between the chosen variables, PCA also provides a simplified data matrix known as the “component score” (or weightings) matrix.

Eigenvalues greater than one indicate that the respective principal component presents more variance than the original standardized variables; thus, the higher the eigenvalue, the greater the variability (Khanchoul and Saaidia 2017). Based on the results of our analysis, the first three principal components (PC01, PC02, and PC03) showed a total variance of 92.34%.

The Table 9 shows that PC01 is highly correlated with  $F_s$ ,  $C$ ,  $D$ , and  $L_g$  ( $PC01 > 0.90$ ). PC01 also shows satisfactorily correlated value of  $0.75 < PC01 < 0.90$  with  $P_{mc}$ ,  $C_c$ , and  $R_n$  and moderately ( $0.60 < PC01 < 0.75$ ) with  $R_h$ ,  $R_c$ ,  $S_w$ ,  $B_h$ ,  $R_f$ , and  $R_e$ . In general, the PC01 is associated to linear parameters. The PC02 correlated satisfactorily with  $R_c$  while moderately with  $R_f$ , HI,  $S_w$ ,  $B_h$ ,  $A$ , and  $R_n$  indicating that it is associated with the degradation of the watershed over time. The PC03 has a satisfactory correlation with  $D_t$  and moderately with  $A$  and  $R_h$ , and these two variables are associated with the shape of the watershed. On the other hand,  $R_{bmn}$  was not correlated significantly with any principal component.

The Fig 7 shows the circular correlation between principal components by pairwise comparison and the influence of each variable. This figure illustrates that the PC01 and PC02 represent almost 80.46% of inertia (Fig 7a). According to the small angle between vectors and its closeness to the circumference, drainage density ( $D$ ), stream frequency ( $F_s$ ), and mean watershed slope ( $P_{mc}$ ) are positively well represented by PC01. On the other hand, the length of overland flow ( $L_g$ ), constant of channel maintenance ( $C$ ), and shape index ( $S_w$ ) show a high negative correlation with PC01. Based on Fig 7b, most of the variables were correlated with PC01,

**Table 8** Eigenvalues explained variability and principal component loadings

Principal component	Eigenvalue	% total variance	Cumulative eigenvalue	% cumulative variance
PC01	8.9865	52.8621	8.9865	52.8621
PC02	4.6917	27.5982	13.6783	80.4603
PC03	2.0194	11.8787	15.6976	92.3390
PC04	0.6535	3.8443	16.3512	96.1833
PC05	0.4210	2.4764	16.7721	98.6597
PC06	0.1616	0.9507	16.9338	99.6104
PC07	0.0662	0.3896	17.0000	100.0000

**Table 9** Correlations between variables and factors (factor loadings)

Variable	PC01	PC02	PC03	PC04	PC05	PC06	PC07
<i>A</i>	-0.237	-0.643	0.696	-0.109	0.036	0.175	0.047
<i>D</i>	<b>0.928</b>	-0.292	-0.200	0.026	-0.090	0.055	-0.050
<i>F<sub>s</sub></i>	<b>0.934</b>	-0.172	-0.020	0.210	-0.074	0.187	-0.118
<i>D<sub>t</sub></i>	0.404	-0.443	<b>0.794</b>	0.061	0.065	-0.027	0.047
<i>F<sub>f</sub></i>	0.638	0.744	0.126	0.015	-0.129	0.065	0.040
<i>R<sub>c</sub></i>	0.634	<b>0.755</b>	0.059	0.020	-0.139	0.020	0.058
<i>R<sub>c</sub></i>	0.710	0.492	0.399	-0.287	-0.023	-0.106	0.005
<i>R<sub>bm</sub></i>	-0.571	0.597	-0.163	-0.421	0.302	0.132	-0.075
<i>R<sub>n</sub></i>	0.759	-0.618	-0.129	-0.048	0.096	-0.110	-0.030
<i>R<sub>h</sub></i>	0.748	-0.103	-0.623	-0.143	0.070	0.080	0.100
<i>L<sub>g</sub></i>	-0.922	0.334	0.004	0.126	-0.007	-0.134	-0.062
<i>C</i>	-0.930	0.327	0.091	0.040	0.120	0.012	0.062
<i>C<sub>c</sub></i>	-0.801	-0.344	-0.351	0.335	0.015	0.033	0.061
<i>B<sub>h</sub></i>	0.689	-0.686	-0.047	-0.112	0.146	-0.131	-0.036
<i>HI</i>	0.375	0.739	0.317	0.368	0.269	0.010	-0.066
<i>P<sub>mc</sub></i>	0.890	0.093	-0.123	0.179	0.381	-0.009	0.079
<i>S<sub>w</sub></i>	-0.703	-0.699	0.074	-0.024	0.078	0.064	-0.022

except the watershed area (*A*) and the drainage texture (*D<sub>t</sub>*); those variables were better represented by PC03.

Comparing PC02 and PC03 (Fig 7c), most of the analyzed variables are not correlated with both principal components, but watershed area (*A*) and drainage texture (*D<sub>t</sub>*) showed a high positive correlation with PC03. The hypsometric integral (*HI*) and elongation ratio (*R<sub>c</sub>*) were the most positively correlated with PC02.

Principal components analysis was used for all morphometric parameters to reduce the information contained in all variables, identify patterns, analyze the relationship between parameters, and therefore to reduce the data of the morphometric parameters influencing the sub-basin evolutions the most and that are related to erosion and degradation processes (Khanchoul and Saaidia 2017). In our study, PCA was useful to regroup parameters with physical significance and discriminate morphometric parameters with lower influence.

The results of this study reveal that PC01 is related to linear parameters, PC02 to watershed shape, and PC03 to relief. The first component values for our watersheds suggests that runoff yield and soil loss can be associated with linear parameters like drainage density (*D*) and stream frequency (*F<sub>s</sub>*). Our results align with what Kamberis et al. (2012) found; *D* and *F<sub>s</sub>* are parameters highly correlated with components like soil texture, land cover, and geology.

### Watershed prioritization

Based on the maximum values among three principal components, variables used to determine watershed prioritization

(Table 10) were stream frequency (*F<sub>s</sub>*), drainage density (*D*), elongation ratio (*R<sub>c</sub>*), and drainage texture (*D<sub>t</sub>*).

We calculated the priority rank (*NP*) according to the watershed degradation degree evaluated for each selected variable and considering the compound parameter (*CP*) as described in the methodology section and classified by priority degree (GP).

To review the importance of the morphometric parameters on watershed degradation and its impact on vegetation cover, the NDVI was used to compare both results and obtain more precise values. Table 10 shows the variations in priority as a function of vegetation cover, where watersheds 01, 03, and 06 decrease their priority rank due to high values of vegetation cover, specifically in the high vegetation class. On the other hand, watersheds 02 and 05 increase their priority rank due to the presence of the urban areas where vegetation cover is scarce and there are large paved areas (Fig 8).

The results of combining the morphometric parameters and vegetation cover estimated with NDVI are presented in Table 10. The morphometry and NDVI describe the watershed degradation caused by water concentrated in the channels and the overland flow on hillslopes, respectively. The use of morphometric parameters and NDVI together, generates a spatial distribution of the general degradation in the watershed and which is useful to define the best management practices for soil and water conservation on streams and hillslopes. Table 10 shows the priority rank for the watersheds as a function of morphometric and NDVI variables; it also shows the final priority combining both procedures.

There is a clear definition among the priority ranks of the watersheds, where the highest priority for intervention is located in the upper areas of the sub-basin, specifically on watersheds 07, 08, and 06. The priority rank indicates the sub-basin degradation condition. In the upper areas, there are steeper lands and deeper channel profiles. As the channels descends along the watershed (Fig 9), the slope or steepness of lands, the depth of the channels, and degradation conditions reduce too. The watershed 01 is classified as high priority by the morphometry component and low priority by NDVI component, but when both components (morphometry and NDVI) are combined, it can be classified as of medium priority. The difference in classification obeys to larger vegetation cover and shows the importance of biomass to control degradation.

In our study, the first-three highly prioritized watershed was found in the upper part of the sub-basin reflecting the importance of linear and shape parameters. Linear and shape parameters combined with heavy rainfalls, steeper slopes, and soils susceptible to water erosion have been generating changes in the evolution of the landscape. In our results, the watersheds that are classified as medium priority (01, 03, and 05) have vegetation cover values greater than the 60% and are even higher than values for

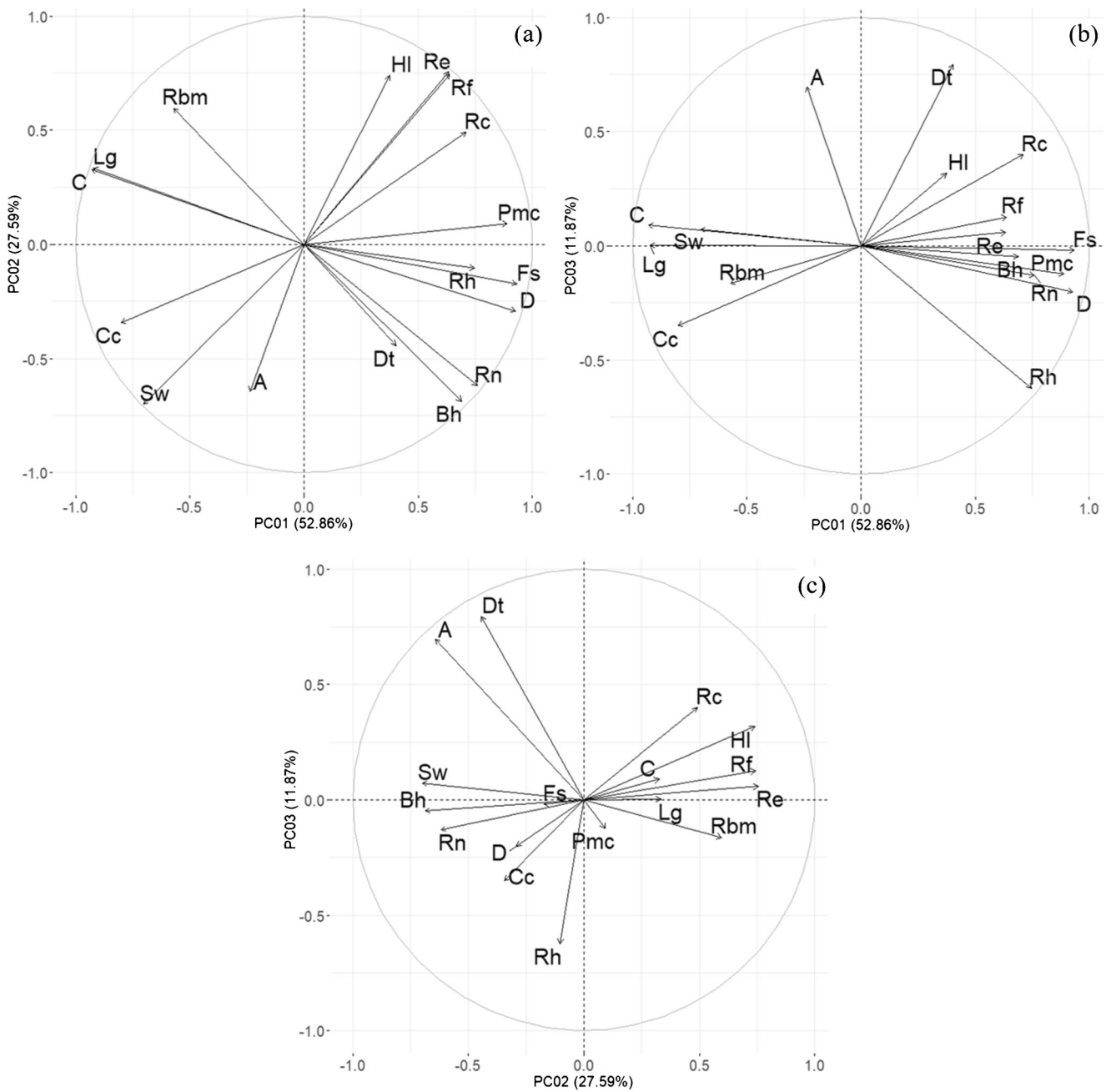


Fig. 7 Circular correlation between variables analyzed and the first three principal components

a watershed classified with high priority. The NDVI classes show that vegetation cover plays an important role on the effects against soil erosion and sub-basin degradation (Table 10). Watersheds with low priority in our research (02 and 04) are spatially distributed in the lower part of the sub-basin, mainly in plain areas with mean elevation values of these two watersheds of 246 and 529 m above mean sea level (Table 4). For the watersheds 02 and 04, the low relief has an important role on the response of the drainage network, and it affects the degradation of the

sub-basin causing frequent flooding and affecting agricultural and urban areas.

### Conclusions

In this study, seventeen morphometric parameters coupled with NDVI of eight watersheds located in Huehuetan river sub-basin of Chiapas, Mexico, were chosen for the watershed prioritization through principal component analysis. The



**Table 10** Watershed prioritization based on both components and final priority

Watershed	Morphometry							NDVI, year 2018								CP <sub>f</sub>	NP <sub>f</sub>	GP <sub>f</sub>			
	F <sub>s</sub>	D	R <sub>e</sub>	D <sub>t</sub>	CP <sub>m</sub>	NP <sub>m</sub>	GP <sub>m</sub>	BS Area		LV Area		MV Area		HV Area					CP <sub>NDVI</sub>	NP <sub>NDVI</sub>	GP <sub>NDVI</sub>
								%	Pr	%	Pr	%	Pr	%	Pr						
1	6	6	1	2	3.75	4	High	0.03	8	0.38	8	37.41	4	62.18	4	6.00	8	Low	4.88	6	Medium
2	7	8	2	8	6.25	7	Low	0.64	5	3.39	4	41.16	2	54.81	6	4.25	4	Medium	5.25	7	Low
3	5	5	3	4	4.25	5	Medium	0.27	6	1.18	6	30.53	6	68.02	3	5.25	6	Low	4.75	5	Medium
4	6	7	8	5	6.50	8	Low	0.07	7	0.50	7	24.36	8	75.07	1	5.75	7	Low	6.13	8	Low
5	4	4	5	6	4.75	6	Medium	1.22	3	3.39	3	33.82	5	61.56	5	4.00	3	High	4.38	4	Medium
6	2	1	4	7	3.50	3	High	0.74	4	2.74	5	27.08	7	69.44	2	4.50	5	Medium	4.00	3	High
7	1	2	6	3	3.00	1	High	7.20	1	7.43	1	40.98	3	44.01	8	3.25	2	High	3.13	1	High
8	3	3	7	1	3.50	2	High	2.25	2	6.46	2	42.47	1	48.81	7	3.00	1	High	3.25	2	High

Where  $F_s$  stream frequency,  $D$  drainage density,  $R_e$  elongation ratio,  $D_t$  drainage texture,  $BS$  bare soil,  $LV$  low vegetation,  $VM$  medium vegetation,  $HV$  high vegetation,  $CP$  compound parameter,  $NP$  priority rank,  $GP$  priority degree,  $Pr$  priority on each class. Sub-indexes  $m$ ,  $NDVI$ , and  $f$  mean morphometry,  $NDVI$ , and final, respectively

component loading matrix obtained from correlation matrix showed that the first three components (PC01, PC02, and PC03) whose Eigenvalues are greater than one together

account for 92.34% of the total explained variance. Based on our results, the first component is strongly correlated with linear parameters, the second component is strongly correlated

**Fig. 8** Spatial variation of NDVI classes in the Huehuetan river sub-basin

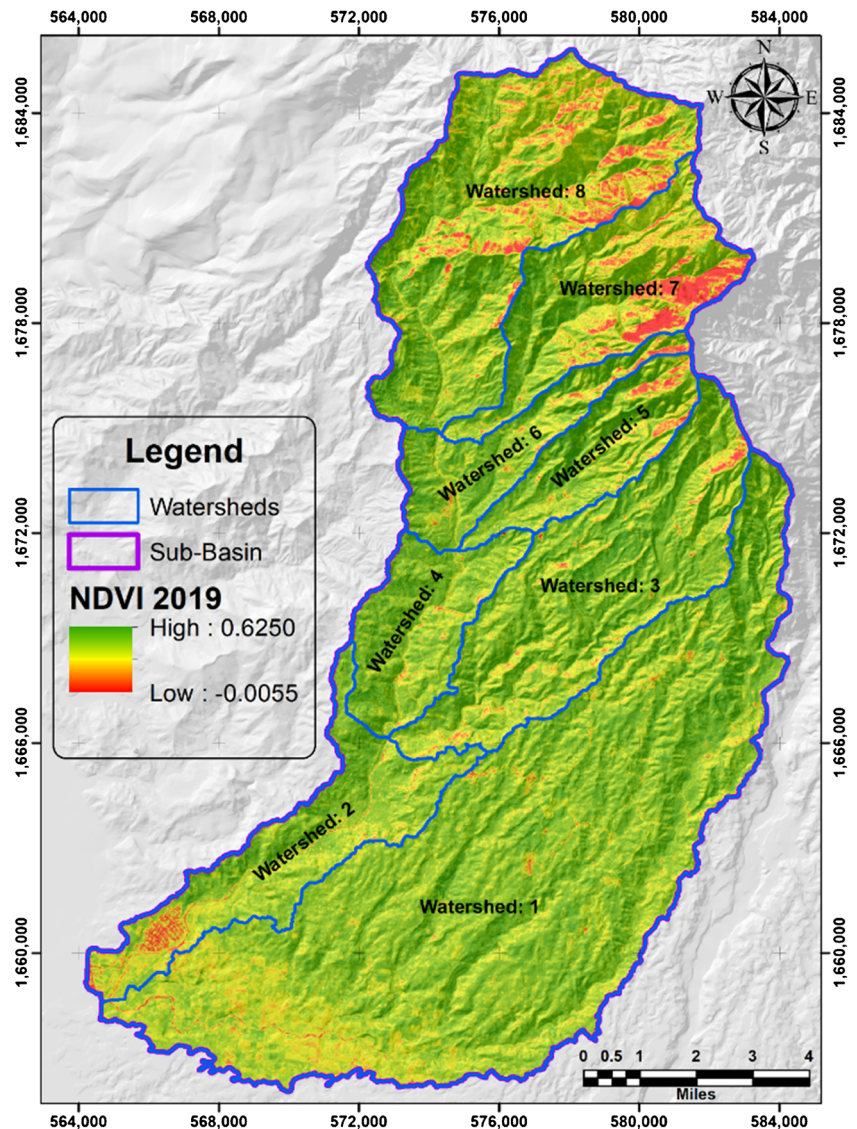
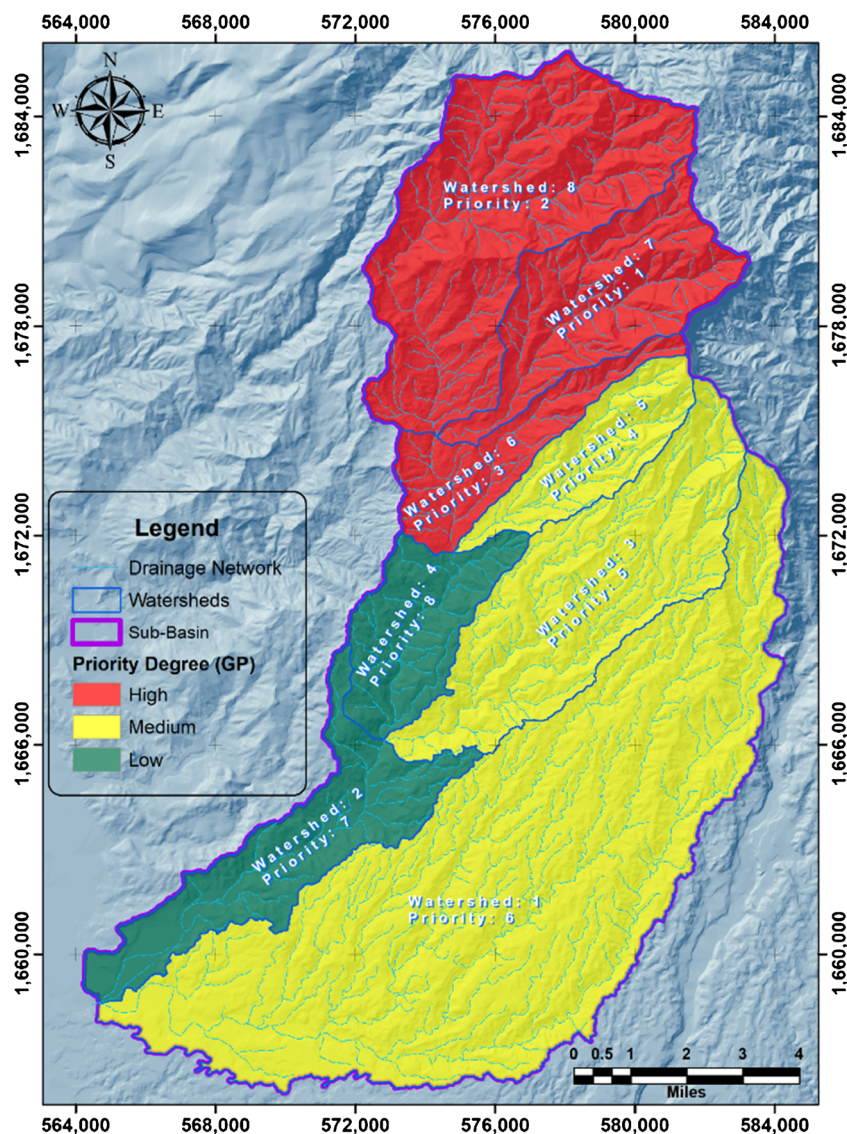


**Fig. 9** Final prioritization of watersheds based on the combination of morphometry and NDVI components



with watershed shape, and the last one (PC03) is associated with relief. Based on the values of the morphometric parameters, three principal components were selected and defined as linear, shape, and relief components. Moreover, we can infer that in hydrological modelling processes such as runoff and sediment yield from small watersheds, our methodology could be useful to discriminate insignificant parameters without losing quality in the results. In addition, the use of both morphometric parameters and NDVI components improves quality watershed prioritization results.

We conclude that it is feasible to analyze fewer variables representing greater variance, as we showed with our methodology and the case we presented in this paper. Otherwise, if the analysis is run with more traditional methods such as weighted sum or multicriteria analysis, a high number of combinations between variable pairs will be required. The present study reveals that parameters related to drainage network ( $F_s$

and  $D$ ) and watershed shape ( $R_c$  and  $D_c$ ) have a great influence on erosive processes of the Huehuetan river sub-basin; all these variables are associated with runoff-erosion processes on channels and drainage network dissection degree. The morphometric analysis allows inferring from basin susceptibility to degradation, and it is an indicator of the potential growth of the drainage system. On the other hand, when NDVI is confronted with morphometric analysis, this index functions as an indicator of the degree of soil protection by vegetation cover. The combination of both components (morphometric parameters and NDVI) to generate a final priority allows identifying the activities needed to mitigate processes of watershed erosion at streams and hillslopes. In this way, areas with higher degradation potential (i.e., sites with greater slopes and higher reliefs) are located in the upper part of the sub-basin, e.g., watershed 07, 08, and 06, for our research. This methodology (morphometric parameters and NDVI

coupled with PCA) helps to reduce analysis time, maintain parameters variability, reduce morphometric parameters on analysis, improve basin public policies, and help decision-makers to implement the best management practices on those areas with greater degradation susceptibility on soil and land use change. The use of PCA for watershed prioritization is a good tool for discriminating the insignificant parameters from the analysis and improves quality of results.

**Acknowledgements** We are grateful to the editor and the anonymous reviewers for their critical review and constructive comments.

**Author contribution** Not applicable

**Data availability** Not applicable

**Code availability** Not applicable

## Declarations

**Conflict of interest** The authors declare that they have no competing interests.

## References

- Abboud IA, Nofal RA (2017) Morphometric analysis of wadi Khumal basin, western coast of Saudi Arabia, using remote sensing and GIS techniques. *J Afr Earth Sci* 126:58–74. <https://doi.org/10.1016/j.jafrearsci.2016.11.024>
- Aher PD, Adinarayana J, Gorantiwar SD (2014) Quantification of morphometric characterization and prioritization for management planning in semi-arid tropics of India: a remote sensing and GIS approach. *J Hydrol* 511:850–860. <https://doi.org/10.1016/j.jhydrol.2014.02.028>
- Ahmed R, Sajjad H, Husain I (2018) Morphometric parameters-based prioritization of sub-watersheds using fuzzy analytical hierarchy process: a case study of lower Barpani Watershed, India. *Nat Resour Res* 27:67–75. <https://doi.org/10.1007/s11053-017-9337-4>
- Al-Saady YI, Al-Suhail QA, Al-Tawash BS, Othman AA (2016) Drainage network extraction and morphometric analysis using remote sensing and GIS mapping techniques (Lesser Zab River Basin, Iraq and Iran). *Environ Earth Sci* 75:1243. <https://doi.org/10.1007/s12665-016-6038-y>
- Altaf F, Meraj G, Romshoo SA (2013) Morphometric analysis to infer hydrological behaviour of Lidder Watershed, Western Himalaya, India. *Geogr J* 2013:1–14. <https://doi.org/10.1155/2013/178021>
- Ansari ZR, Rao LAK, Yusuf A (2012) GIS based morphometric analysis of Yamuna Drainage Network in parts of the Fatehabad area of Agra District, Uttar Pradesh. *J Geol Soc India* 79:505–514. <https://doi.org/10.1007/s12594-012-0075-2>
- Babu KJ, Sreekumar S, Aslam A (2016) Implication of drainage basin parameters of a tropical river basin of South India. *Appl Water Sci* 6:67–75. <https://doi.org/10.1007/s13201-014-0212-8>
- Baumann J, Arellano MJL (2003) Measuring rainfall erosivity characteristics and annual R-factors adjustment of the USLE in tropical climate. In: Gabriel D, Cornelis W (eds) *25 years of assessment of erosion. Proceedings of the International Conference*. Ghent University, Belgium, pp 67–74
- Bishop MP, Shroder JF, Bonk R, Olsenholler J (2002) Geomorphic change in high mountains: a western Himalayan perspective. *Glob Planet Chang* 32:311–329. [https://doi.org/10.1016/S0921-8181\(02\)00073-5](https://doi.org/10.1016/S0921-8181(02)00073-5)
- Biswas S, Sudhakar S, Desai VR (1999) Prioritisation of subwatersheds based on morphometric analysis of drainage basin: a remote sensing and GIS approach. *J Indian Soc Remote* 27(3):155–166. <https://doi.org/10.1007/BF02991569>
- Chandniha SK, Kansal ML (2017) Prioritization of sub-watersheds based on morphometric analysis using geospatial technique in Piperiya watershed, India. *Appl Water Sci* 7(1):329–338. <https://doi.org/10.1007/s13201-014-0248-9>
- Chauhan P, Chauniyal DD, Singh N, Tiwari RK (2016) Quantitative geomorphometric and land cover-based micro-watershed prioritization in the Tons river basin of the lesser Himalaya. *Environ Earth Sci* 75(6):498. <https://doi.org/10.1007/s12665-016-5342-x>
- Chopra R, Dhiman RD, Sharma PK (2005) Morphometric analysis of sub-watersheds in Gurudaspur district, Punjab using remote sensing and GIS techniques. *J Indian Soc Remote* 33(4):531–539. <https://doi.org/10.1007/BF02990738>
- Chowdary VM, Chakraborty D, Jeyaram A, Krishna-Murthy YVN, Sharma JR, Dadhwal VK (2013) Multi-Criteria Decision Making Approach for Watershed Prioritization Using Analytic Hierarchy Process Technique and GIS. *Water Resour Manag* 27:3555–3571. <https://doi.org/10.1007/s11269-013-0364-6>
- Dash P, Aggarwal SP, Verma N (2013) Correlation based morphometric analysis to understand drainage basin evolution: a case study of Sirva River Basin, Western Himalaya, India. *Scientific Annals of "Alexandru Ioan Cuza" University of Iasi. Geography Series* 59(1):35–58
- Eze BE, Efiog J (2010) Morphometric parameters of the Calabar River Basin: implication for hydrological processes. *J Geograp Geol* 2(1):18–26. <https://doi.org/10.5539/jgg.v2n1p18>
- Farhan Y, Anbar A, Al-Shaikh N, Mousa R (2017) Prioritization of semi-arid agricultural watershed using morphometric and principal component analysis, remote sensing, and GIS techniques, the Zerqa River Watershed, Northern Jordan. *Agric Sci* 8:113–148. <https://doi.org/10.4236/as.2017.81009>
- Gómez-Almonte MK (2005) Índice de Vegetación en Áreas del Bosque Seco del Noroeste del Perú a Partir de Imágenes Satelitales. Universidad de Piura, Perú, Dissertation, pp 131
- Gopinath G, Nair AG, Ambili GK, Swetha TV (2016) Watershed prioritization based on morphometric analysis coupled with multi criteria decision making. *Arab J Geosci* 9:129. <https://doi.org/10.1007/s12517-015-2238-0>
- Gravelius H (1914) *Flusskunde*. Goschen Verlagshan dlug Berlin. In: Zavoianu I (1985) *Morphometry of Drainage Basins*. Amsterdam, Elsevier, pp 237
- Gupta R, Misra AK, Sahu V (2019) Identification of watershed preference management areas under water quality and scarcity constraints: case of Jhajjar district watershed, India. *Appl Water Sci* 9:27. <https://doi.org/10.1007/s13201-019-0905-0>
- Hajam RA, Hamid A, Dar NA, Bhat SU (2013) Morphometric analysis of Vishav drainage basin using geo-spatial technology (GST). *Int Res J Geol Min* 3(3):136–146
- Harlin JM (1978) Statistical moments of the hypsometric curves and its density function. *Math Geol* 10(1):59–72
- Horton RE (1945) Erosional development of streams and their drainage basins: a hydrophysical approach to quantitative morphology. *Geol Soc Am Bull* 56:275–370. <https://doi.org/10.1007/BF01033300>
- Horton RE (1932) Drainage basins characteristics. *Trans Am Geophys Union* 13:350–361. <https://doi.org/10.1029/TR013i001p00350>
- Howard AD (1990) Role of hypsometry and planform in basin hydrologic response. *Hydrol Process* 4(4):373–785. <https://doi.org/10.1002/hyp.3360040407>

- Javed A, Khanday MY, Ahmed R (2009) Prioritization of subwatersheds based on morphometric and land use analysis using remote sensing and GIS techniques. *J Indian Soc Remote* 37:261–274. <https://doi.org/10.1007/s12524-009-0016-8>
- Joji VS, Nair ASK, Baiju KV (2013) Drainage basin delineation and quantitative analysis of Panamaram Watershed of Kabani River Basin, Kerala using remote sensing and GIS. *J Geol Soc India* 82(4):368–378. <https://doi.org/10.1007/s12594-013-0164-x>
- Kamberis E, Bathrellos GD, Kokinou E, Skilodimou HD (2012) Correlation between the structural pattern and the development of the hydrographic network in a portion of the Western Thessaly Basin (Greece). *Cent Eur J Geosci* 4(3):416–424. <https://doi.org/10.2478/s13533-011-0074-7>
- Kanth TA, Hassan Z (2012) Morphometric analysis and prioritization of watersheds for soil and water resource management in Wular catchment using geo-spatial tools. *Int J Geol Agric Environ Sci* 2(1):30–41
- Khanchoul K, Saaidia B (2017) Morphometric analysis of river subwatersheds using geographic information system and principal component analysis, northeast of Algeria. *Revista de Geomorfologie* 19:155–172. <https://doi.org/10.21094/rg.2017.018>
- Kouli M, Vallianatos F, Soupios P, Alexakis D (2007) GIS-based morphometric analysis of two major watersheds, Western Crete, Greece. *J Environ Hydrol* 15:1–17
- Kumar S, Chaudhary BS (2016) GIS applications in morphometric analysis of Koshalya-Jhajarhara watershed in Northwestern India. *J Geol Soc India* 88:585–592. <https://doi.org/10.1007/s12594-016-0524-4>
- Kusre BC (2016) Morphometric analysis of Diyung Watershed in Northeast India using GIS technique for flood management. *J Geol Soc India* 87:361–369. <https://doi.org/10.1007/s12594-016-0403-z>
- Lê S, Josse J, Husson F (2008) FactoMineR: An R package for multivariate analysis. *J Stat Softw* 25(1):1–18. <https://doi.org/10.18637/jss.v025.i01>
- Londhe S, Nathawat MS, Subudhi AP (2010) Erosion, susceptibility zoning and prioritization of mini-watersheds using geomatics approach. *Int J Geom Geosci* 1(3):511–528
- Lykoudi E, Angelaki M (2004) The contribution of the morphometric parameters of a hydrologic network to the investigation of the neotectonic activity: an application to the upper Acheloos River. *Bull Geol Soc Greece* 36:1084–1092. <https://doi.org/10.12681/bgsg.16913>
- Mahala A (2020) The significance of morphometric analysis to understand the hydrological and morphological characteristics in two different morpho-climatic settings. *Appl Water Sci* 10(33):01–16. <https://doi.org/10.1007/s13201-019-1118-2>
- Magesh NS, Chandrasekar N, Soundranagayam JP (2011) Morphometric evaluation of Papanasam and Manimuthar watersheds, parts of Western Ghats, Tirunelveli district, Tamil Nadu, India: a GIS approach. *Environ Earth Sci* 64:373–381. <https://doi.org/10.1007/s12665-010-0860-4>
- Magesh NS, Jitheshlall KV, Chandrasekar N, Jini KV (2013) Geographical information system-based morphometric analysis of Bharathapuzha river basin, Kerala, India. *Appl Water Sci* 3(2):467–477. <https://doi.org/10.1007/s13201-013-0095-0>
- Magesh NS, Chandrasekar N (2012) GIS model-based morphometric evaluation of Tamiraparani subbasin, Tirunelveli district, Tamil Nadu, India. *Arab J Geosci* 7:131–141. <https://doi.org/10.1007/s12517-012-0742-z>
- Maurya S, Srivastava PK, Gupta M, Islam T, Han D (2016) Integrating soil hydraulic parameter and microwave precipitation with morphometric analysis for watershed prioritization. *Water Resour Manag* 30:5385–5405. <https://doi.org/10.1007/s11269-016-1494-4>
- Martínez-Ramírez A, Steinich B, Tuxpan J (2017) Morphometric and hypsometric analysis in the Tierra Nueva Basin, San Luis Potosí, México. *Environ Earth Sci* 76:444. <https://doi.org/10.1007/s12665-017-6766-7>
- Méndez WJ (2016) Análisis cuantitativo del relieve en cuencas de drenaje de la vertiente norte del macizo “El Ávila” (estado de Vargas, Venezuela) y su significado geomorfológico. *Investigaciones Geográficas, Instituto de Geografía, UNAM, Mexico* 91:25–42. <https://doi.org/10.14350/ig.47722>
- Merg C, Petri D, Bodoira F, Nini M, Fernández M, Schmidt F, Montalva R, Guzmán L, Rodríguez K, Blanco F, Selzer F (2011) Mapas digitales regionales de lluvias, índice estandarizado de precipitación e índice verde. *Revista Pilquen, Sección Agronomía* 13(11):1–11
- Meshram SG, Sharma SK (2018) Application of principal component analysis for grouping of morphometric parameters and prioritization of watershed. In: Singh V, Yadav S, Yadava R (eds) *Hydrologic Modeling*. Water Science and Technology Library, vol 81. Springer, Singapore. [https://doi.org/10.1007/978-981-10-5801-1\\_31](https://doi.org/10.1007/978-981-10-5801-1_31)
- Mígiros G, Bathrellos GD, Skilodimou HD, Karamousalis T (2011) Pinios (Peneus) river (Central Greece): hydrological – geomorphological elements and changes during the quaternary. *Cent Eur J Geosci* 3(2):215–228. <https://doi.org/10.2478/s13533-011-0019-1>
- Miller V (1953) A quantitative geomorphic study of drainage basin characteristics in the Clinch Mountain Area, Virginia and Tennessee. Project NR 389-402, Technical Report 3, Columbia University, Department of Geology, New York, pp 51
- Mishra SS, Nagarajan R (2010) Morphometric analysis and prioritization of sub-watersheds using GIS and Remote Sensing techniques: a case study of Odisha, India. *Int J Geom Geosci* 1(3):501–510
- Nag SK (1998) Morphometric analysis using remote sensing techniques in the Chaka sub-basin, Purulia district, West Bengal. *J Indian Soc Remote* 26(1):69–76. <https://doi.org/10.1007/BF03007341>
- Nag SK, Chakraborty S (2003) Influence of rock types and structures in the development of drainage network in hard rock area. *J Indian Soc Remote* 31:25–35. <https://doi.org/10.1007/BF03030749>
- Olguín-López JL, Pineda-López R (2010) Importance of hydrological prioritization in management decision making in the sub-basin of the Ayuquila river, Jalisco, México (*In Spanish*). *CIENCIA@UAQ* 3(2):42–51
- Pal B, Samanta S, Pal DK (2012) Morphometric and hydrological analysis and mapping for Watut watershed using remote sensing and GIS techniques. *Int J Adv Eng Technol* 1:357–368
- Patel DP, Dholakia M, Naresh N, Srivastava PK (2012) Water harvesting structure positioning by using geo-visualization concept and prioritization of mini-watersheds through morphometric analysis in the lower Tapi basin. *J Indian Soc Remote* 40(2):299–312. <https://doi.org/10.1007/s12524-011-0147-6>
- Pérez-Peña JV, Azañón JM, Azor A (2009) CalHypso: An ArcGIS extension to calculate hypsometric curves and their statistical moments. Application to drainage basin analysis in SE Spain. *Computers & Geosciences* 35:1214–1223. <https://doi.org/10.1016/j.cageo.2008.06.006>
- Phani RP (2014) Morphometry and its implications to stream sediment sampling: a study on Wajrakarur Kimberlite field, Penna river basin, Anantapur district, Andhra Pradesh, India. *Int J Geomatics Geosci* 5(1):74–90
- Prabhakar AK, Singh KK, Lohani AK, Chandniha SK (2019) Study of Champua watershed for management of resources by using morphometric analysis and satellite imagery. *Appl Water Sci* 9:127. <https://doi.org/10.1007/s13201-019-1003-z>
- Price K (2011) Effects of watershed topography, soils, land use, and climate on baseflow hydrology in humid regions: a review. *Prog Phys Geogr* 35(4):465–492. <https://doi.org/10.1177/0309133311402714>
- Prieto-Amparán JA, Pinedo-Alvarez A, Vázquez-Quintero G, Valles-Aragón MC, Rascón-Ramos AE, Martínez-Salvador M, Villarreal-Guerrero F (2019) A multivariate geomorphometric approach to

- prioritize erosion-prone watersheds. *Sustainability* 11(18):5140. <https://doi.org/10.1177/0309133311402714>
- Racca JMG (2007) Análisis hipsométrico, frecuencia altimétrica y pendientes medias a partir de modelos digitales del terreno. *Boletín del Instituto de Fisiografía y Geología* 77(1-2):31–38
- Rai PK, Mohan K, Mishra S, Ahmad A, Mishra VN (2017) A GIS-based approach in drainage morphometric analysis of Kanhar River Basin, India. *Appl Water Sci* 7:217–232. <https://doi.org/10.1007/s13201-014-0238-y>
- Rakesh K, Lohani AK, Sanjay K, Chatterjee C, Nema RK (2000) GIS based morphometric analysis of Ajay river basin up to Sarath gauging site of South Bijar. *J Appl Hydrol* 14(4):45–54
- Ramaiah SN, Gopalakrishna GS, Vittala SS, Najeeb KM (2012) Morphometric analysis of sub-basins in and around Malur Taluk, Kolar District, Karnataka using remote sensing and GIS techniques. *Nat Environ Pollut Technol* 11(1):89–94
- Ramu B, Mahalingam B (2012) Hypsometric properties of drainage basins in Karnataka using geographical information system. *New York Sci J* 5(12):156–158
- Ratnam KN, Srivastava Y, Rao VV, Amminedu E, Murthy K (2005) Check dam positioning by prioritization of micro-watersheds using SYI model and morphometric analysis-remote sensing and GIS perspective. *J Indian Soc Remote Sens* 33:25–38. <https://doi.org/10.1007/BF02989988>
- Resmi MR, Babeesh C, Achyuthan H (2019) Quantitative analysis of the drainage and morphometric characteristics of the Palar River basin, Southern Peninsular India; using bAd calculator (bearing azimuth and drainage) and GIS. *Geology, Ecology, and Landscapes* 3(4): 295–307. <https://doi.org/10.1080/24749508.2018.1563750>
- Rudraiah M, Govindaiah S, Vittala SS (2008) Morphometry using remote sensing and GIS techniques in the sub-basins of Kagna river basin, Gulburga District, Karnataka, India. *J Indian Soc Remote* 36:351–360. <https://doi.org/10.1007/s12524-008-0035-x>
- Samal DR, Gedam SS, Nagarajan R (2015) GIS based drainage morphometry and its influence on hydrology in parts of Western Ghats region, Maharashtra, India. *Geocarto Int* 30(7):755–778. <https://doi.org/10.1080/10106049.2014.978903>
- Schumm SA (1956) Evolution of drainage systems and slopes in Badlands at Perth Amboy, New Jersey. *Geol Soc Am Bull* 67(5): 597–646. [https://doi.org/10.1130/0016-7606\(1956\)67\[597:eodas\]2.0.co;2](https://doi.org/10.1130/0016-7606(1956)67[597:eodas]2.0.co;2)
- Sharma SK, Gajbhiye S, Tignath S (2015) Application of principal component analysis in grouping geomorphic parameters of a watershed for hydrological modeling. *Appl Water Sci* 5:89–96. <https://doi.org/10.1007/s13201-014-0170-1>
- Singh P, Gupta A, Singh M (2014) Hydrological inferences from watershed analysis for water resource management using remote sensing and GIS techniques. *Egypt J Remote Sens Space Sci* 17(2):111–121. <https://doi.org/10.1016/j.ejrs.2014.09.003>
- Singh V, Dubey A (2012) Linear aspects of Naina-Gorma river basin morphometry, Rewa district, Madhya Pradesh, India. *Int J Geom Geosci* 3(2):364–372
- Singh S, Singh MC (1997) Morphometric analysis of Kanhar River Basin. *Natl Geogr J India* 43:31–43
- Singh V, Singh UC (2011) Basin morphometry of Maingra River, district Gwalior, Madhya Pradesh, India. *Int J Geom Geosci* 1(4):891–902
- Singh PK, Kumar V, Purohit RC, Kothari M, Dashora PK (2009) Application of principal component analysis in grouping geomorphic parameters for hydrologic modeling. *Water Resour Manag* 23: 325–339. <https://doi.org/10.1007/s13201-014-0170-1>
- Smith KG (1950) Standards for grading textures of erosional topography. *Am J Sci* 248:655–668
- Sreedevi PD, Subrahmanyam K, Ahmed S (2005) The significance of morphometric analysis for obtaining groundwater potential zones in a structurally controlled terrain. *Environ Geol* 47:412–420. <https://doi.org/10.1007/s00254-004-1166-1>
- Strahler AN (1952) Hypsometric (area-altitude) analysis of erosional topography. *Geol Soc Am Bull* 63:1117–1142. [https://doi.org/10.1130/0016-7606\(1952\)63\[1117:HAAOET\]2.0.CO;2](https://doi.org/10.1130/0016-7606(1952)63[1117:HAAOET]2.0.CO;2)
- Strahler AN (1957) Quantitative analysis of watershed geomorphology. *Trans Am Geophys Union* 38:913–920. <https://doi.org/10.1029/TR038i006p00913>
- Strahler AN (1964) Quantitative geomorphology of drainage basin and channel network. In: Chow VT (ed) *Handbook of Applied Hydrology*. McGraw Hill Book Company, New York, pp 39–76
- Tolessa GA, Rao PJ (2013) Watershed development prioritization of Tandava river basin, Andhra Pradesh, India - GIS approach. *Int J Eng Sci Invent* 2(2):12–20
- Verdin KL, Verdin JP (1999) A topological system for delineation and codification of the Earth's river basins. *J Hydrol* 218(1-2):1–12. [https://doi.org/10.1016/S0022-1694\(99\)00011-6](https://doi.org/10.1016/S0022-1694(99)00011-6)
- Vincy MV, Rajan B, Pradeepkumar AP (2012) Geographic information system-based morphometric characterization of sub-watersheds of Meenachil river basin, Kottayam district, Kerala, India. *Geocarto Int* 27(8):661–684. <https://doi.org/10.1080/10106049.2012.657694>
- Vittala SS, Govindaiah S, Gowda HH (2004) Morphometric analysis of sub-watersheds in the Pavagada area of Tumkur district, South India using remote sensing and GIS techniques. *J Indian Soc Remote* 32(4):351–362. <https://doi.org/10.1007/BF03030860>
- Zarco-Arista AE, Espinosa-García AC, Mazari-Hiriart M (2010) Riesgo potencial de las actividades del sector económico sobre la biodiversidad y la salud humana. In: Cotler H (ed) *Las Cuencas Hidrográficas de México Diagnóstico y Priorización*, 1st edn. Instituto Nacional de Ecología, México, pp 112–119